Journal Pre-proof

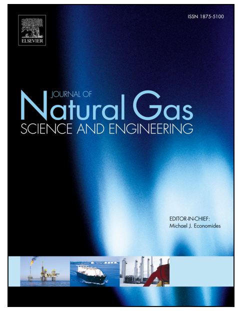

A review on gas hydrate production feasibility for permafrost and marine hydrates

Patrick Edward Chibura, Wei Zhang, Anjian Luo, Jinjie Wang

PII: S1875-5100(22)00035-X

DOI: https://doi.org/10.1016/j.jngse.2022.104441

Reference: JNGSE 104441

To appear in: *Journal of Natural Gas Science and Engineering*

Received Date: 26 August 2021

Revised Date: 7 January 2022

Accepted Date: 24 January 2022

A Review on Gas Hydrate Production Feasibility for Permafrost and Marine Hydrates

Patrick Edward Chibura [a, c], Wei Zhang[b], Anjian Luo[a], Jinjie Wang [a, *]

[a] Key Laboratory of Tectonics and Petroleum Resources (China University of Geosciences), Ministry of Education, Wuhan, 430074, China.

[b] Exploration and Development Research Institute of TuHa Oilfield Company, CNPC, Hami, 839000, China.

[c] Chemistry Department, University of Dar es Salaam, P.O. Box 35061 Dar es Salaam, Tanzania.

*Corresponding author: wangjinjie06-2@163.com

Abstract

Methane gas hydrate is a potential energy reserve that would supplement the current energy supply in the world. This study presents a review of methane hydrate production through various simulations and field trial tests. The simulated production data of three classes of gas hydrate reservoirs were evaluated and compared. In line with that, factors such as porosity, permeability, gas saturation, pressure, temperature, surface area were discussed and analyzed. It was revealed that in all methane hydrate reservoirs classes, production factors such as injection rate, temperature, and pressure drop, as well as reservoir parameters suit of permeability, porosity, and surface area show substantial gas production. On the contrary, CMG STARS and TOUGH+HYDRATE have better prediction results than other studied simulators. Methane hydrate reservoirs classes 1, 2, and 3, depressurization and thermal techniques have a recovery rate of 75% and 49.06%, respectively while CO_2 injections and combination methods have a recovery rate of 64%, and 87.5%. Reformation of hydrate near the wellbore, sand production, the rise of bottom well pressure, and geomechanical effects are methane production challenges

Keywords: Methane hydrate: reservoir simulation: hydrate reservoirs: methane recovering methods: production parameters: field case production.

1. Introduction

Gas hydrate was first reported in 1811 (Davy, 1811), whereas hydrates clogged oil and gas pipelines were first published in 1934 (Hammerschmidt, 1934). It is found in permafrost (areas with the permanently frozen ground) 0 - 900 m depths and marine regions in depths ranging from 300–500 m (Makogon, 1965, Bily and Dick, 1974, Sloan and Koh, 1998). Worldwide, the quantity of carbon found in methane hydrates is approximate twice the amount of fossil fuel reserves in the globe (Collett, 2001, Walsh, Hancock, 2009). Thus, the extraction of methane from hydrates is considered a promising way to resolve potential shortages of energy in the world. Methane hydrates are crystalline clathrates formed by water and gas interactions at relatively low temperatures and high pressures. (Vysniauskas and Bishnoi, 1983, Kim, Bishnoi, 1987). The formation of methane hydrate is an exothermic process that releases heat while the decomposition of hydrate into gas and water is an endothermic process (Zhao, Cheng, 2012).

Natural gas hydrates are mostly composed of methane, however other components such as hydrocarbons, H_2S, and CO_2 have been discovered in high-pressure and low-temperature gas hydrates. (Makogon, 2010). After decomposition, 1 m^3 of hydrates yields 164 m^3 of gas and 0.8 m^3 of water (Makogon and Omelchenko, 2013). Natural gas exploration from methane hydrate is considered an important energy source due to the increase in energy demand in the world. However, the study and exploitation of methane hydrate have always presented economic challenges (Moridis, Silpngarmlert, 2011, Ruppel, 2011). Field tests trial was done in a different area in the world but faces many challenges (Makogon and Omelchenko, 2013, Kurihara, Sato, 2010, Garapati, McGuire, 2013, Konno, Fujii, 2017, Yamamoto, Terao, 2014, Chen, Feng, 2018a, Chen, Feng, 2018b). Such challenges that have limited the full exploration of methane gas hydrate include sand production together with methane, the rise of bottom well pressure, geomechanical effects, reformation of gas hydrate near the wellbore, and so on.

Different numeric reservoir simulators are developed to model the methane production of gas hydrate, among them are TOUGH+HYDRATE (Moridis, Kowalsky, 2005a), MH-21 (Oyama and Masutani, 2017), HydrateResSim (Moridis, Kowalsky, 2005b, Moridis, Kowalsky, 2005c), CMG-STARS (Stars, 2007), STOMP (White and Oostrom, 2006). This review compares hydrate production feasibility based on reservoir simulation in different reservoirs. In addition, a few field case studies are discussed. This review is presented in the following layout: first is an introduction of the study, and distribution, second classification, methods of production gas hydrate, experimental production, numerical simulation prediction of methane production. This is followed by field case production, and finally is the conclusion of the study.

1.1 Distribution of Gas Hydrate

Estimates of methane hydrate levels in permafrost and oceanic deposits range from 1.4 x 10^{13} to 3.4 x 10^{16} m^3 and 3.1 x 10^{15} to 7.6 x 10^{18} m^3, respectively (Kvenvolden, 1988). Figure 1 is a map showing areas where gas hydrate has been recovered, where gas hydrate is considered to be present. Based on seismic evidence, gas hydrate drilling expeditions in permafrost or deep marine environments have been conducted and often have contributed to gas hydrate recovery. Globally gas hydrate supplies are valued at between 2.83 x 10^{13} to 8.5 x 10^{13} m^3 (Collett, 2001, Makogon, Holditch, 2007). Approximately, 99% of the world's methane hydrate is found in marine deposits at depths of 300 to over 2500m (Kumar and Linga, 2017).

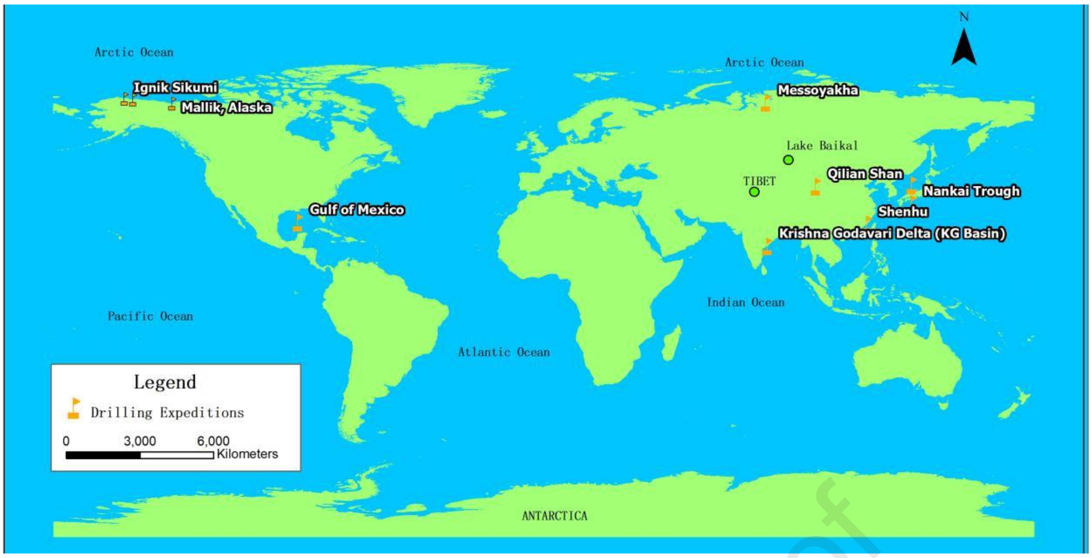

Figure 1. Map of gas hydrate drilling in the world.

1.1.1 Permafrost gas hydrates

Permafrost is about 20% of the northern hemisphere's land area and is associated with the onshore and nearshore gas hydrate reserves. Permafrost deposit data are of good quality due to comparatively easier access and signifies a large share of the whole hydrate database. Four permafrost reserves are under consideration in the world as targets for development, first is (a) *Mackenzie Delta, Canada Mallik Methane Hydrate Deposits*. The approximate volume of methane hydrates in the accumulations of hydrate is about 2.8 x 10^{10} - 2.8 x 10^{11} m^3 at standard temperature and pressure (STP) that makes the Mallik area be most concentrated methane hydrates accumulations in the world (Majorowicz and Osadetz, 2001, Osadetz and Chen, 2005). (b) *Deposit of Alaska's Northern part, Eileen USA methane hydrate*. Several publications detail the geology and geochemistry of rocks on the northern slope of Alaska and the measurement of the sub-surface temperature needed to evaluate the stability of methane hydrate distribution (Bird and Magoon, 1987, Collett, 1993). The amount of methane hydrate in the Eileen methane hydrate deposit is about 1.0 x 10^{12} - 1.2 x 10^{12} m^3 STP (Collett, 2007). Collett (Collett, 1993) estimated double the amount of identified conventional gas at a field of the Prudhoe Bay area. (c) *West Siberia, Russia the Messoyakha area with 24 x 10^9 m^3 methane* *hydrates reserves.* The Messoyakha area of the north slope in the West Siberian Basin remains an example of a deposit of gas hydrates that had already been commercially extracted. It is approximated that 36% (5 *x* 10^{9} m^3 STP) of the overall gas output comes from gas hydrates (Makogon, 1981). (d) *Qilian Mountains, China, with permafrost area 1 x 10^{11} m^2* (ZHU, ZHANG, 2010) this form of methane is described as having a thinner permafrost zone, a shallower buried depth, a more complicated gas component, and a coal-bed origin. Also, high electrical resistivity and sonic velocity are also seen in the logging profile.

1.1.2 Oceanic Deposits / Marine Hydrate

Owing to the higher cost of deep-water activities, the problems facing the commercialization of marine hydrate are possibly greater than the amount in the Arctic. The following are examples of Marine Hydrate: Offshore Japan-Nankai Trough, which was the first offshore natural hydrate discovery undertaken in Japan. The presence of hydrate in pore spaces of several layers of sand between 1135 and 1213 m was recognized (Takahashi, Yonezawa, 2001). Although the net amount of the hydrate at this location was very limited, a method was established for quantifying the hydrate in the deepwater sediment. Takahashi and Tsuji (Takahashi and Tsuji, 2005) conducted a multi-well development project at 16 locations in three separate sites selected under the bottom simulating reflector signature at 720 - 2033 m water depths. 32 wells were drilled and an assessment was carried out (Fujii, Saeki, 2008, Kurihara, Sato, 2008, Saeki, Fujii, 2008).

Gulf of Mexico - Oligocene Frio Formation, Tigershark accumulations, is another example of marine methane hydrate. This is the first recorded high-S_H hydrate-bearing sand described in the Gulf of Mexico at Alaminos Canyon Block 818. Log results from an exploration well are estimated to be 2750 m of site H_2O. Reported that the sandy hydrate-bearing layer (HBL) presence (3210 - 3228 m drilling depth) of 18.25 m thickness at a comparatively high temperature (around 21 °C), a large porosity of approximately 0.30, range of intrinsic permeability, and a stability zone at slightly below the hydrating base of the gas hydrate (Moridis and Reagan, 2007). Preliminary synthetic data simulations show that the gas output level of these systems can well exceed 2.8 x 10^5 m^3.

Shenhu Area, South China Sea (Ye, Qin, 2020) the reservoir occurs in shallow, loose, soft, unconsolidated sediments at a depth of fewer than 400 m beneath the seafloor, where the ocean is more than 800 m deep and sand makes up a minor percentage of the total volume. The depressurization thermal techniques and Horizontal well drilling were used. 30 days of continuous gas production were achieved in the South China Sea's 1225.23 m deep Shenhu Area, with total gas production of 86.14 x 10^4 m^3. As a result, daily gas output averages 2.87 x 10^4 m^3, which is 5.57 times higher than the initial production test of 5 x 10^3 m^3/day.

1.2 Structure of gas hydrates

The three most prevalent crystalline structures of gas hydrates are structure I (sI cubic), structure II (sII cubic), and structure H (sH hexagonal) as shown in Figure 2 (Sloan and Koh, 1998, Sloan and Koh, 2007). The structure I (sI) is a mixture of H_2O and hydrocarbons with a molecular weight less than C_3H_8 as well as various inorganic gases. This contains 46 water molecules and two small pentagonal dodecahedron (5^{12}) cavities with a radius of 3.95, which can be occupied by CH_4 with a stabilized crystal size of 4.36, and six large tetrakaidecahedron ($5^{12}6^2$) cavities with an average radius of 4.33, which fit for smaller molecules than 6 in diameter, such as CO_2 (5.12) (Sloan and Koh, 2007, McMullan and Jeffrey, 1965). Structure II (sII) is larger than ethane but smaller than pentane, containing 136 water molecules and 16 small (5^{12}) and 8 large hexakaidecahedron ($5^{12}6^4$) cavities with sizes ranging from 6–7 (McMullan and Jeffrey, 1965). Structure H (sH) comprises 34 H_2O containing 3 smaller (5^{12}) cavities, 2 small ($4^3 5^6 6^3$) cavities, and 1 large ($5^{12}6^8$) cavities (Ripmeester, John, 1987).

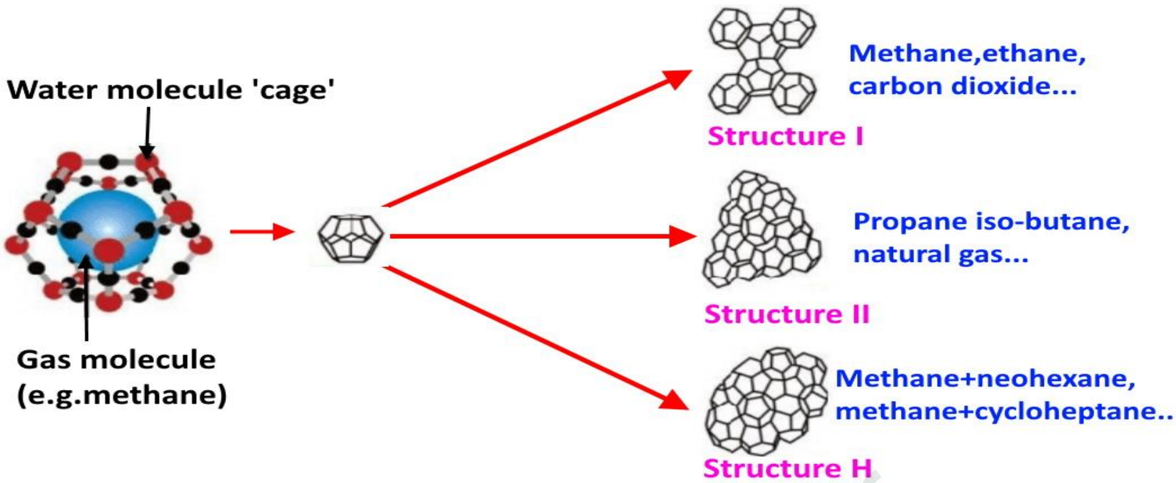

Figure 2. Hydrate structures: sI, sII, and Sh modified from (Sloan Jr ED, Koh CA 2008).

2. Classification and Production Methods for methane from methane hydrates

2.1 Four Class of Gas Hydrates Reservoirs

Deposits of methane hydrates are classified into four principal groups (Table 1 and Figure 3) which are class 1, class 2, class 3, and class 4 building on basic geological features and the conditions of the initial reservoir (Moridis and Collett, 2003, Moridis, 2008).

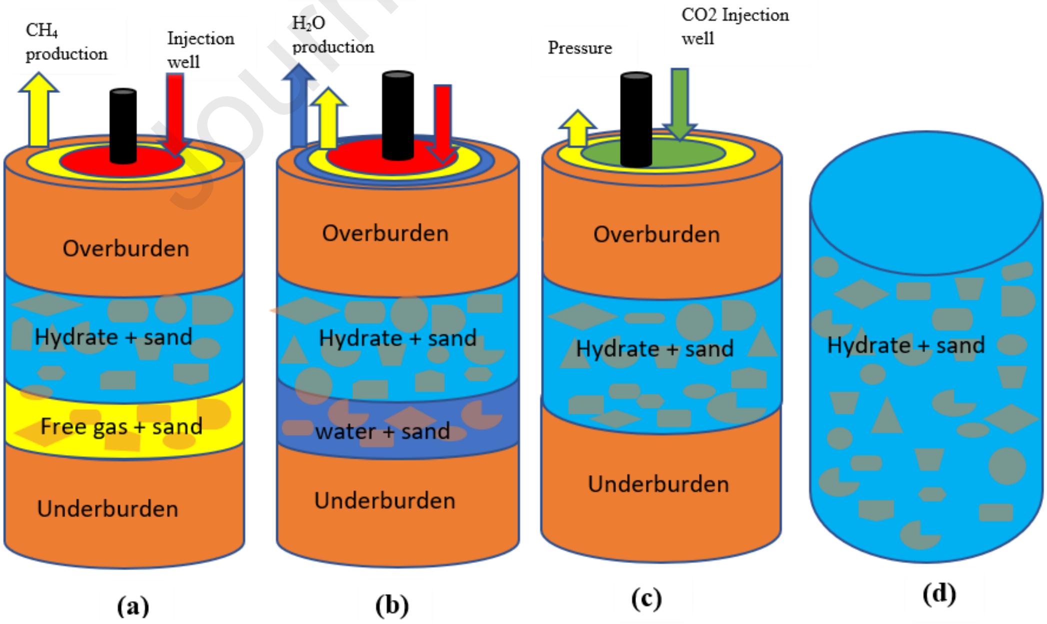

Figure 3. Hydrate Deposit: (a) Class 1, (b) Class 2, (c) Class 3, (d) Class 4 modified (Moridis and Collett, 2003, Moridis and Sloan, 2007).

Table 1

Four Classes, Features, and Examples of Hydrate Reservoir

Class	Features	Examples	Reference
1	-Contain overburden, hydrate, free gas, and underburden layers -sandstones and carbonate rocks	Mallik field in Canada's Mackenzie Delta, Eileen field in Russia's North Slope, Alaska, USA, and Messoyakha site in West Siberia. Nankai Trough offshore in Japan and offshore in the Gulf of Mexico	(Moridis and Collett, 2003, Moridis, 2008, Moridis, Kowalsky, 2007, Bhade and Phirani, 2015, Kurihara, Ouchi, 2011, Lin, Sukru)
2	- Comprise overburden, hydrate, water, and underburden layers -formations of fractures/vugs -sandstones and carbonate rocks	Mallik site, Eastern Nankai trough, Ulleung Basin East Sea Korea and Shenhu in China	(Lin, Sukru, Xu and Li, 2015) (Kurihara, Ouchi, 2011, Su, He, 2012)
3	-contains overburden, hydrate, and underburden layers -sandstones and carbonate rocks	Qilian Mountain permafrost in China	(Bhade and Phirani, 2015, Lin, Sukru). (Kurihara, Ouchi, 2011).

4	- No geological strata -sandstones and carbonate rocks - containing scattered -low-saturation hydrate (S_H < 10%)	Krishna Godavari basin in India, Gulf of Mexico in the USA	(Moridis and Sloan, 2007, Bhade and Phirani, 2015, Lin, Sukru, Xu and Li, 2015, Konno, Masuda, 2010)

2.2 Methods of Production methane from methane hydrates

Methane is produced from methane hydrates by depressurization [9, 57-70, thermal (Holder, Angert, 1982, Bayles, Sawyer, 1986, Selim and Sloan, 1989, Selim and Sloan, 1990, Ullerich, Selim, 1987, Tsypkin, 1992, Tsypkin, 2001, Xu, 2004, Islam, 1994, Jamaluddin, Kalogerakis, 1989, Merey and Longinos, 2018a), Chemical Injection(Sung, Lee, 2002, Kamath, Mutalik, 1991, Kamath and Godbole, 1987), CO_2 Swapping (Merey and Longinos, 2018a, Ohgaki, Takano, 1996, Nakano, Yamamoto, 1998, Smith, Seshadri, 2001, McGrail, Zhu, 2004, Ota, Morohashi, 2005, White and McGrail, 2008, Deusner, Bigalke, 2012, Handa, 1986, Kang, Lee, 2001, Janicki, Schlüter, 2014, Duan, Gu, 2016, Merey, Al-Raoush, 2018), or a combination of either method. But depressurization has become more common due to many advantages to all classes of methane hydrate reservoirs. To summarize the methods identified to recover methane from the below-discussed class Table 2 presents advantages and conditions involved for every respective process.

Table 2

Comparison production methods of methane from methane hydrates

Methods	Action	Advantages	Disadvantages	References

Depressurization	Decreases the pressure beneath the hydrate balance.	Is cheaper than thermal stimulation due to endothermal,	-Slow in production, sand production, geomechanical risks.	(Kim, Bishnoi, 1987, Merey and Longinos, 2018a, Yousif, Abass, 1991, Yousif and Sloan, 1991, Sung, Huh, 2000, Goel, Wiggins, 2001, Khataniar, Kamath, 2002, Ahmadi, Ji, 2004, Hong and Pooladi-Darvish, 2003, Hong and Pooladi-Darvish, 2005, Ji, Ahmadi, 2001, Ji, Ahmadi, 2003, Bai, Zhang, 2012, Zhao,

				Zhu, 2015, Moridis, 2002)
Thermal Stimulation	Increasing temperature above the temperature of the hydrate equilibrium.	Simple, renewable, rapid, easy to control, high efficiency, no pollution.	Is expensive due to the amount of energy needed, the heat lost in non-hydrated sections, and low injection rates, weather-sensitive, kill aquatic animals.	(Holder, Angert, 1982, Bayles, Sawyer, 1986, Selim and Sloan, 1989, Selim and Sloan, 1990, Ullerich, Selim, 1987, Tsypkin, 1992, Tsypkin, 2001, Xu, 2004, Islam, 1994, Jamaluddin, Kalogerakis, 1989, Merey and Longinos, 2018a)

Chemical Injection	Lower permeability of hydrate-bearing regions by Salts, alcohols, and glycols.	Low energy injection, simple and convenient due to shifting the hydrate equilibrium between pressure and temperature, resulting in a rapid dissociation of gas hydrates.	Is very expensive, the reaction is slow and inefficient dissociation of hydrate in the reservoir, causes pollution in the environment.	(Sung, Lee, 2002, Kamath, Mutalik, 1991, Kamath and Godbole, 1987)
CO_2 Swapping	Due to Molecular structure and size, quadruple moment, and diffusion rate, CH_4 is replaced by CO_2.	Reduced geomechanical hazards, lower water output, low injection rate, and low replacement rate are all factors that influence competitive adsorption. CO_2 storage is	CO_2 hydrate that forms prevents further interaction between the CO_2 and CH_4 hydrates, preventing methane hydrate dissociation.	(Merey and Longinos, 2018a, Ohgaki, Takano, 1996, Nakano, Yamamoto, 1998, Smith, Seshadri, 2001, McGrail, Zhu, 2004, Ota, Morohashi, 2005, White and

	The heat required to create CO_2 hydrate (57.9 kJ/mol) is more than the heat required to dissociate CH_4 hydrate (54.5 kJ/mol) in an exothermic reaction.	important for environmental conservation.	Due to the poor effective permeability of gas hydrates and the sluggish rate of replacement, the injection rate is slow.	McGrail, 2008, Deusner, Bigalke, 2012, Handa, 1986, Kang, Lee, 2001, Janicki, Schlüter, 2014, Duan, Gu, 2016, Merey, Al-Raoush, 2018)

2.3 Experimental production

Many studies have been reported on laboratory productions of methane from methane hydrate reservoirs. (Zhao, Liu, 2020) Fine marine sediments hinder the synthesis of methane, resulting in an uncontrolled pressure decrease and gas emission, according to laboratory studies on methane production performance from methane hydrate reservoirs sediments by depressurization. In addition, gradual depressurization causes a temperature reduction in the reservoir, which leads to rehydration formation. (Liang, Yang, 2021) studied the reaction rate constant of hydrate formation by using X-ray. From $5.3\ 10^{7}$ to $1.65\ 10^{6}$ m/s, the reaction rate constant increased as the temperature raised. Also, experiments carried by (Vysniauskas and Bishnoi, 1983) show that temperatures change from 274 to 284 K, with pressures change from 3 to 10 MPa affects the hydrate equilibrium curve. (Ruan and Li, 2021) compared experimental and computational data on the effect of methane hydrate surface area in porous surfaces on depressurization-induced methane dissociation. After numerical simulations and laboratory work under the same series of conditions, the surface area of hydrate is expressed as a function of porosity, hydrate saturation, and average diameter of sediment particles (Nakayama, Sato, 2007). Also, a study by (Lee, Seo, 2003) reports 64% CH_4 to recover from class 3 methane hydrate reservoir when CO_2 is injected. Although much work has been done, further research should be done on reservoir permeability, preventing sand production in conjunction with methane, controlling bottom well pressure, and controlling gas hydrate reformation near the wellbore.

3. Numerical simulation

A numerical simulation is a computer-based calculation that uses a program to implement a mathematical model of a physical system (Zakharov, Dyachenko, 2002). Because their mathematical models are too complex to provide analytical answers, most nonlinear systems require numerical simulations to analyze their behavior. Reservoir simulation is a computer technique to model the fluid flow in porous media over a period of time. Such simulators are focused on considering both fluid flow and heat transfer while presuming the solid phase is immobile. The simulator is based on various scientific models that describe the petrophysical characteristics of a deposit. Various simulators are developed and various methods are used to model the dissociation actions of the gas hydrate (Swinkels and Drenth, 2000). Studies reported on simulation of methane hydrate reservoir production that deals with the solution of a complex combination of highly coupled fluid, heat, and mass transport equations combined with the potential for the formation and/or disappearance of multiple solid phases in the system (Wilder, Moridis, 2008). Numerical simulation depends on (1) the existence of vigorous simulators describing the processes that dominate (2) Awareness of the parameters and their relationships that determine all components of the simulated scheme's physical processes and thermophysical properties (3) Accessibility of field and laboratory data for the validation of a numerical model (Wilder, Moridis, 2008, Sun, Wang, 2019). Also, the equilibrium model, thermal conductivity model, Kinetic model, Permeability model, and mechanical model were reported on the numerical model by (Ruan, Li, 2021). Each of the five simulators has an equilibrium and kinetic model for hydrate production and dissociation (Moridis, Kowalsky, 2005b, Moridis, Kowalsky, 2005c, White and Oostrom, 2006, Moridis, 2014a, CMG, 2015, Kurihara, Ouchi, 2004, Moridis, Kowalsky, 2005d, White, 2006). But each simulator work under specific assumptions and conditions. The equilibrium hydration model accounts for heat as well as up to four mass components, namely H_2O, CH_4, and water-soluble inhibitors like salts or alcohols; the kinetic model adds the fifth component, the CH_4-hydrate, which is now treated as a separate component rather than a state of the H_2O-CH_4 system (Moridis, 2014a). The hydrate dissociation reaction is expected to proceed at equilibrium in simulation (Moridis, 2014a). The viability of hydrate production in different reservoirs is compared using reservoir simulations that look at various characteristics like permeability, porosity, temperature, pressure drops, surface area, injection rate, and well pattern.

Table 3

Different simulator

Model name and Capabilities	Factors	Equations	Simulator	References
equilibrium and kinetic model	The Mass and Energy Balance Equation	$\frac{d}{dt}\int_{V\eta} M^k \, dV = \int_{T\eta} F^k \cdot \eta \, d\Gamma + \int_{V\eta} q^k \, dV$ 1	TOUGH+HYDRATE	(Moridis, Kowalsky, 2005a, Moridis, Kowalsky, 2008, Moridis, 2014b, Grover, Holditch, 2008, Clarke and Bishnoi,
	Mass Accumulation Terms	Equilibrium Model $m^k = \sum_{B\equiv A,G,I} \Phi s_\beta \rho_\beta x_\beta^k, k \equiv w, m, i$ … … … … … 2 Kinetic Model $m^k = \sum_{\beta\equiv A,G,H,I} \Phi s_\beta \rho_\beta x_\beta^k, k \equiv w, m, h, i$ … … … … 3		
	Heat Accumulation Terms	$M^\theta = (1-\emptyset)\rho_R C_R T + \sum_{B=A,G,H,I} \emptyset \, S_\beta \rho_\beta \bigcup_\beta + Q_{diss}$ ....4 $Q_{diss} = \begin{cases} \Delta(\emptyset^{\rho_H S_H} \Delta H^0) \; for \; equilibrium \\ Q_H \Delta H^0 \; for \; kinetic \end{cases}$ … … … 5		
	Clarke and kim-Bishnoi	$n_H(t) = n_0 - \frac{\pi}{\psi} v \left(\frac{1}{3}\mu_0^0 G^2 t^3 + \mu_1^0 G t^2 + \mu_2^0 t\right) x \sum_j K d_f (f_{eq} - f_g^v) j, ave,$ … … 6 But $G = -\frac{M}{3\rho}\frac{\pi}{\Phi_v}\frac{s}{\Psi}\left(\frac{6\Phi_v}{\pi}\right)^{\frac{2}{3}} \sum_j K d_f (f_{eq} - f_g^v) j, ave,$		

Model name and Capabilities	Factors	Equations	Simulator	References
	Source and Sink Terms	$\hat{q}^k = \sum_{k\equiv A,G} X_\beta^k q_\beta \,, k \equiv w, m \ldots\ldots 7$ Equilibrium $\hat{q}^\theta = q_d + \sum_{k\equiv A,G} h_\beta q_\beta \ldots\ldots\ldots 8$ Kinetic $\hat{q}^\theta = q_d + \sum_{k\equiv A,G} h_\beta q_\beta + Q_H \Delta H^0 \ldots\ldots 9$		2001a, Clarke and Bishnoi, 2001b)
	absolute permeability Relative permeability	$k_{ra} = min\left\{\left[\frac{S_a - S_{ira}}{1 - S_{ira}}\right]^n, 1\right\} \ldots\ldots 10$ $k_{rG} = min\left\{\left[\frac{S_G - S_{irG}}{1 - S_{ira}}\right]^n, 1\right\} \ldots\ldots 11$		
	inhibitor	$U_A = X_A^w u_A^w + X_A^m\,(u_A^m + U_{sol}^m) + X_A^i(u_A^i + U_{sol}^i) \ldots\ldots 12$		
Equilibrium and Kinetic Model (CH_4 hydrate)	mass and heat balance	$\frac{d}{dt}\int_{Vn} M^k\,dV = \int_{\tau n} F^k \cdot nd_\tau + \int_{V_n} qk\,dV \ldots\ldots 13$	HydrateResSim	(Moridis, Kowalsky, 2005b, Moridis,
	mass accumulation terms	$m^k = \sum_{B\equiv A,G,I} \phi S_\beta \rho_\beta x_\beta^k \ldots\ldots 14$		
	Heat accumulation term	$M^h = (1-\emptyset) P_R c_R T + \sum_{\beta\equiv A,G,H,I} \emptyset\, S_\beta \rho_\beta \bigcup_\beta + \emptyset\, P_H \Delta s_H \Delta H^0 \ldots\ldots 15$		

Model name and Capabilities	Factors	Equations	Simulator	References
	Mass flux	$F^{k}=\sum_{B\equiv A,G} F_{\beta}^{k} \ldots\ldots\ldots\ldots 16$		Kowalsky, 2005c)
Equilibrium and Kinetic Model Model (CH_4-CO2 mixed hydrate)	Energy conservation	2 $\frac{\partial}{\partial t}\left(\sum_{1=l,g,n,h,i,p}(\boldsymbol{\phi\rho_{\gamma}s_{\gamma}u_{\gamma}})+(\mathbf{1}-\emptyset)\boldsymbol{P_s u_s}\right)=-\sum_{y=l}\boldsymbol{l\nabla}(\boldsymbol{h_y Fy'})-\sum_{\varsigma=w,a,o}\left(\boldsymbol{\nabla C_g^{h^{\varsigma}} J_g^{\varsigma}}\mathbf{1}-\boldsymbol{\nabla}(\boldsymbol{k_R\nabla T})\right)+\sum_{Y=l,g,n}(\boldsymbol{h_y m_y})+\boldsymbol{q} \ldots\ldots\ldots\ldots\ldots\ldots\ldots \mathbf{17}$	STOMP-HYD	(Phale, Zhu, 2006)
	Mass conservation	$\frac{\partial}{\partial t}\left(\sum_{y=l,g,n,h,i,p}\left(\emptyset^{\rho_{\gamma}s_{\gamma}\omega_{\gamma}^{\varsigma}}\right)\right)=-\sum_{y=l,g,n}\left(\nabla\left(\omega_{\gamma}^{\varsigma}F_{\gamma}\right)\right)-\sum_{y=l,g}\left(\nabla\left(J_{\gamma}^{\varsigma}\right)\right)+\sum_{y=l,g,n}\left(\omega_{\gamma}^{\varsigma}m_{\gamma}\right)\ Where\ \varsigma=w,a,o,s \ldots\ldots\ldots\ldots\ldots 18$		
	diffusion-dispersive flux and advective	$F_{\gamma}=\frac{P_{\gamma}k_{r\gamma}k_i}{\mu_{\gamma}}\left(\nabla_{P_y}+\rho_y g z_g\right)\ Where\ \gamma=l.g.n \ldots\ldots\ldots\ldots\ldots\ldots .19$		
	Diffusive mass flux	$J_y^{\varsigma}=-\emptyset^{\tau}\gamma^{P}\gamma^{5}\gamma\frac{m^{\varsigma}}{m^{\gamma}}\cdot D_{\gamma}^{\varsigma}\left(\nabla x_{\gamma}^{\varsigma}\right)\ for\ \gamma=l\ and\ \varsigma=w,a,o,s \quad for\ \gamma=g\ and\ \varsigma=w,a,o \ldots\ldots 20$		
	Heat balance	$H_B=(T_0-T_{\theta B})\left(C_r(1-\emptyset)+C_{h^{\emptyset}}S_{hO}+Cw^{\emptyset}S_{wO}\right) \ldots\ldots\ldots\ldots\ldots\ldots\ldots 21$	MH-21 HYDRES	

Model name and Capabilities	Factors	Equations	Simulator	References
Equilibrium and Kinetic Model (CH_4 hydrate)	initial saturation MH layer absolute permeability relative permeability	$Sho-opt=\frac{(T_{\theta O}-T_{\theta B})(C_{\gamma}(1-\emptyset)+Cw^{\emptyset})}{\emptyset^{[\Delta H+(T_{\theta O}-T_{\theta B}-\Delta T_{\theta})(C_h-C_w)]}}\ldots\ldots\ldots\ldots\ldots\ldots.22$ $k_D=k_{D0}(1-S_H)^N\ldots\ldots.23$ $k_{rg}=k_r g^0(1-Se)\ldots\ldots24$ $Where$ $S_e=\frac{S_{wm}-S_{iw}}{1-S_{ig}-S_{iw}}$		(Sasaki, Sugai, 2014, Kurihara, 2005).
Equilibrium and Kinetic Model (CH_4/CO_2 hydrates)	Rate of hydrate formation	$\frac{dC_H}{dt}\Big\vert_{Form}=A\cdot\exp\left(-\frac{E}{RT}\right)(\phi S_a\rho_a)(\phi S_H\rho_H)(y_i p_g)\left(1-\frac{1}{k(R,T)}\right)\ldots\ldots\ldots\ldots24$	CMG STARS	(Stars, 2007, CMG, 2015, CMG, 2017)
	Rate of hydrate decomposition	$\frac{dC_H}{dt}\Big\vert_{Decomp}=B(1+\phi S_H)\cdot\exp\left(-\frac{E}{RT}\right)(\phi S_a P_a)(y_i p_g)\left(1-\frac{1}{k(R,T)}\right)\ldots\ldots\ldots\ldots25$		
Kim-Bishnoi	Kinetic Force equilibrium.	$\frac{dCH}{dt}=k_d A_d(p_e-P_g)\ldots\ldots\ldots\ldots26$ Kinetic model $r_k=\lim\cdot\exp\left(-E_a{}^k/_{RT}\right)\cdot\prod_{i=l}^{n_c}c_i^e k$ Where $C_i=\varphi_f\rho_j S_j x_{j_i}\quad j=w,o,g\ldots\ldots\ldots\ldots\ldots.27$ $\nabla\cdot\sigma-B=0\ldots\ldots\ldots.28$		(Kim, Bishnoi, 1987, Lin and Hsieh, 2020, Wu

Model name and Capabilities	Factors	Equations	Simulator	References
Geomechanical Model	Strain-displacement relation. Total and effective stress relation.	$\varepsilon = {}^{1}/_{2}\,(\nabla u + (\nabla u)^{T})\ \ldots\ldots\ldots\ldots\ldots 29$ $\sigma = \sigma' + \alpha p I\ \ldots\ldots\ldots\ldots\ldots..30$		and Hsieh, 2020)

221

3.1 **Simulating methane production from class 1 methane hydrate reservoirs**

TOUGH+HYDRATE (T + H) is a gas hydrate simulator, with code FORTRAN 95/2003 (Moridis, Kowalsky, 2005a, Zhang, 2009). This simulator incorporates models that describe mass and energy balance, mass accumulation, heat accumulation, fluid flow, source and sink, and inhibitor (Table 3) (Moridis, 2014b, Moridis and Kowalsky, 2006a). All possible mechanisms of hydrate dissociation, such as depressurization, in which the release of gas is accomplished by decreasing the pressure under the stability of methane hydrate, thermal stimulation, in which the release of gas is effected by heating the hydrate above the temperature of dissociation at a specified pressure, salting effects and inhibitor-induced effects, in which the hydrocarbon is generated after injection (Moridis, 2014b, Grover, Holditch, 2008).

(Grover, Holditch, 2008) used (T + H) to predict methane production at Messoyakha reservoir (class 1) by considering depressurization as a primary mechanism for recovering gas. Porosity, absolute permeability, relative permeability, initial gas saturation, capillary pressure, thickness, gas production rate, water saturation, and irreducible water saturation were studied using various TOUGH+HYDRATE equations (Table 3). When other sedimentary materials are kept constant, an increase in permeability and heat flow led to an increase in CH_4 production. Their estimate was 36% of gas produced from hydrates after about 20 years of production. Similarly, studies from (Moridis, Kowalsky, 2007, Moridis and Kowalsky, 2006a, Alp, Parlaktuna, 2007) employed the same simulator and considered factors like porous medium, porosity, relative permeability, capillary pressure, a saturation of gas hydrate, gravity equilibrium, and temperature is studied by different scholars to evaluate their impact on methane production from class 1 methane hydrate reservoir. Permeability (management of gas flow), capillary pressure (pressure drop that disturbs hydrate equilibrium), and heat flow (wellbore control of gas hydrate reformation) are few factors that contribute to CH_4 production from methane hydrate reservoirs. The first is water and hydrate in the hydrate zone (Class 1W), while the second is gas and hydrate in the gas zone (Class 2W) (Class 1G) (Moridis, Kowalsky, 2007). Class 1W hydrates donate up to 65% of the production rate and up to 45 % of the total volume of gas produced, whereas Class 1 G hydrates are 75% and 54%, respectively (Moridis, Kowalsky, 2007, Alp, Parlaktuna, 2007). Class 1 G has a higher production rate than class 1W due to the current accumulation of free gas, which reacts slowly but increases methane productions over time. In addition, a study combining experimental and theoretical results on the influence of surface area on cumulative gas output in methane hydrate porous media by depressurization discovered that the surface area of hydrate dissociation has a significant impact on cumulative gas output (Ruan and Li, 2021). Their findings suggest that the grain-coating surface area model achieves well for hydrate dissociation simulation at lower hydrate saturations, but the hydrate dissociation simulation by Clarke and kim-Bishnoi equation (Clarke and Bishnoi, 2001a, Clarke and Bishnoi, 2001b) helps to calculate hydrate dissociation kinetic reaction. Although the use of the pore-filling surface area model performs better at higher hydrate saturation (Moridis, 2008, Moridis, Kowalsky, 2007). Among all major methods of dissociation, depressurization tends to be ideally suited for class 1 deposit conditions due to its ease, methodological and economic efficiency, and rapid hydrate response to quickly decreasing pressure (Moridis, 2008, Moridis, Kowalsky, 2007). In all these case studies their models assumed 1) Zero salinity because of uncertainty, 2) Early pressure at the hydrate-gas interface and the temperature equilibrium. Despite a promising recovery factor through depressurization in class 1 methane hydrate reservoir, the remaining gas amount in the reservoir suggests the consideration of combination methods with other techniques like thermal, inhibitors to maximize production. Also, more study is needed on the application of dual vertical wells, horizontal wells, and fracking (which increases permeability and improves gas flow) to enhance methane output from methane hydrate reservoirs.

Several studies have utilized the STAR (Steam Thermal and Advanced Processes Reservoir simulator) simulator to investigate methane productions from class 1 methane hydrate reservoirs (Stars, 2007). It is a package in the Computer Modeling Group Limited (CMG) simulator capable of measuring the flow of multiphase fluids, thermal, steam additives, and geomechanical analysis as shown in Table 3 (CMG, 2015, Howe, Patil, 2009). STAR contains the kinetic parameters of the Kim-Bishnoi equation Table 3 (Kim, Bishnoi, 1987) that can establish dissociation of heat and thermodynamic stability of hydrate, which is a core mechanism for hydrate simulation (Howe, 2004).

Considering reservoir and production parameters such as porosity, permeability, pressure, temperature, saturation, wellbore, overburden, underburden, heat flow, CO_2 injection rate, and well bottom-hole pressure, scholars (Walsh, Hancock, 2009, Uddin and Coombe, 2007, Llamedo, Provero, 2010) incorporated a multi-phase and multi-component gas model in the STAR simulator to assess methane production when CO_2 is injected into the hydrate formation. Their findings show that cumulative methane gas produced using thermal and depressurization methods was 3.7 x10^6 m^3 in 8000 days. Also, the result shows that the cumulative methane produced from methane hydrate was 77% while 23% come from free gas in Class 1. (Lin and Hsieh, 2020, Wu and Hsieh, 2020) considered a geomechanics-methane hydrate reaction-multiphase fluid flow model to study the possibility of carbon dioxide enhanced gas recovery (CO_2-EGR) in Class-1 methane hydrate reservoir. In Figure 4 there is also a dramatic drop in methane gas output, which could be attributed to a decrease in free gas available in class one, sand formation, or gas hydrate regeneration in the pipe. Parameters like viscosity, porosity permeability, saturation temperature, pressure stress (σ), strain (ε), and displacement (u) that affect the production of methane were analyzed. It was observed as the pressure drops further towards 70%, the total recovery factor increased towards 64%. In addition, the increase of successful formation stress as the reservoir pore pressure decreased, induces compression in the reservoir rock, resulting in vertical subsidence.

On the other hand, (Bai, Hou, 2020) utilized the STAR simulator by incorporating the impact of the presence of interbeds to evaluate the production of gas hydrate. Interbed model and non-interbed model were used in their analysis. Interbed clay was observed to disrupt the transmission of pressure, temperature, and materials in the class 1 methane hydrate reservoir, and the effect was noticeable to occur mostly near the inflection point of the cumulative methane production curve.

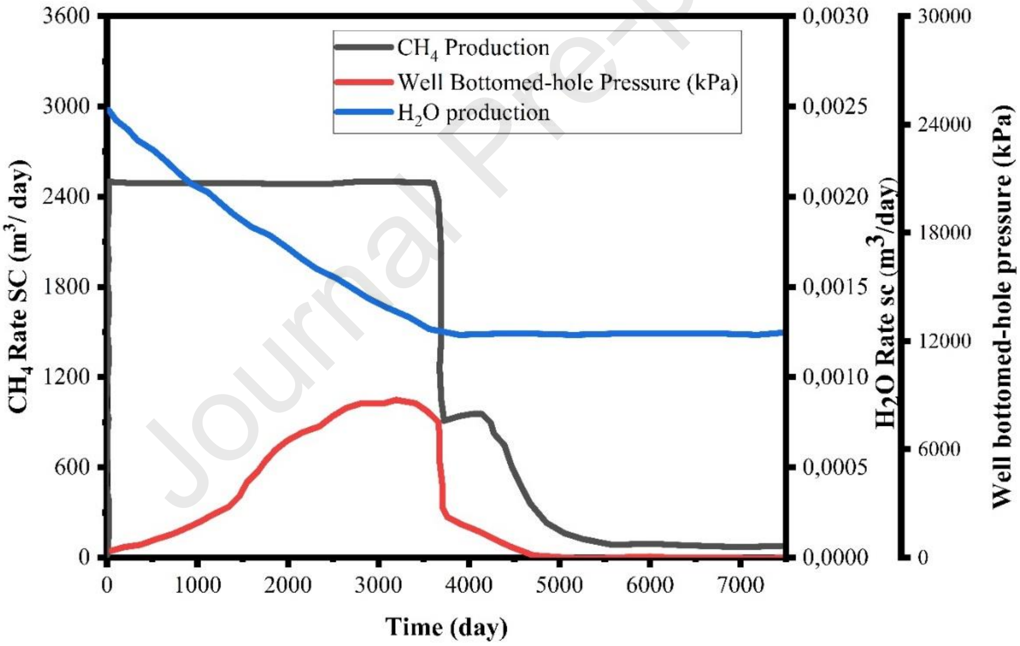

Figure 4. Production of CH_4 in class 1 methane hydrate reservoir by depressurization (*Lin and Hsieh, 2020*)

HydrateResSim (HRS) is another simulator applied to predict methane production from class 1 methane hydrate reservoirs (Moridis, Kowalsky, 2005b, Moridis, Kowalsky, 2005c). HydrateResSim simulations can be sustained by depressurization, thermal injection, and chemical injection techniques. Recovering methane through CO_2/N_2 injection HydrateResSim is modified to Mix3HydrateResSim. The original code (T+H) allows for heat distribution and up to 3 components (H_2O, CH_4, and inhibitors), while the improved code (HydrateResSim) allows for heat distribution and up to 4 components (H_2O, CH_4, CO_2/N_2, and inhibitors) between 4 possible phases (gas, aqueous, ice, and hydrate) (Garapati, McGuire, 2013). HydrateResSim is either performed by employing an equilibrium model and the kinetic model is shown in Table 3. The application of both equilibrium and kinetic models in depressurization with/without wellbore heating methods to predict methane production (Merey and Longinos, 2018a, Merey and Sinayuc, 2016, Merey and Longinos, 2018b). (Garapati, McGuire, 2013) studies simulations by injection of a CO_2 and N_2 mixture on a simple 1-D methane hydrate followed by output using a single well by depressurization. It is observed that CH_4 is released from the hydrate and CO_2/N_2 gases are absorbed to form hydrate whereby hydrate is released during depressurization.

Factors like porosity, permeability, temperature, saturation, relative permeability capillary pressure, the thickness of hydrate, and the thickness of free gas were evaluated. Their results show that more methane is produced when the pressure is reduced, but hydrate reformation along the wellbore during production is prevented by wellbore heating until a certain value is reached. (Liu, Hou, 2019) utilized a modified HydrateResSim that incorporated Kim-Bishinoi kinetic model (Kim, Bishnoi, 1987) and Vysniauskas-Bishinoi kinetic model (Sloan Jr and Fleyfel, 1991). Their simulations considered temperature, pressure, intrinsic permeability, porosity, saturation, geothermal gradient, and Water injection rate. Results show that the cumulative gas output due to depressurization is $2.88\ x\ 10^7$ m^3, while that of geothermal energy-assisted natural (GEAN) maximum approximately up $4.72\ x\ 10^7$ m^3, with an increase of 63.9 %. Despite the good predictions with different production methods, HydrateResSim is not capable of predicting geomechanical changes during gas production because it presumes that sediments are stationary (Merey and Longinos, 2018a).

Furthermore, CH_4 production from Class 1 methane hydrate reservoirs can be simulated by using STOMP-HYD (White and Oostrom, 2006, Phale, Zhu, 2006). STOMP-HYD solves masses of H_2O, CH_4, CO_2, inhibitor (salts or alcohols), and thermal energy equations indicated in Table 3 (White, Wurstner, 2011). Also, STOMP-HYD can distinguish different mobile phases that may exist in the reservoir (such as gas, aqueous, and liquid) and immobile phases (like ice, hydrate, precipitated salt, and geological media). To solve the dominant conservation equations, the STOMP-HYD simulator solves by integral volume differentiation with orthogonal grids for spatial discretization (White, Wurstner, 2011). In the simulation process parameters: pressure, temperature, CO_2-microemulsion injection rate, and the concentration of injected CO_2-microemulsion on methane hydrate dissociation are considered. The injection of CO_2-microemulsion for CH_4 recovery from methane hydrate reservoirs was observed using the multifluid transport equation 17-20 from Table 3 in this work.

Results from on dimension (1-D) simulations show that CO_2-microemulsion injection produces more methane than hot water injection alone, and also show that liquid CO_2-microemulsion injection facilitates the early and substantial production of methane as compared to CO_2-microemulsion vapor injection (Phale, Zhu, 2006). Due to its molecular structure and size, quadruple moment, and diffusion rate, CO_2 has a thermodynamic advantage over CH_4 in hydrates; also, the heat emitted during the creation of CO_2 hydrate is 20% higher than the heat necessary to dissociate CH_4 hydrate (Phale, Zhu, 2006).

(White, Wurstner, 2011, White and McGrail, 2009) used CO_2 swapping considering permeabilities, capillary pressure, porosity, liquid CO_2 effective saturation, gas effective saturation, and aqueous effective saturation. Their findings show that CO_2 injection can only generate methane around 10% of the original reservoir amount after the depressurization stage which is mainly due to the replacement of methane gas saturation in the gas zone. The mechanism of CO_2-CH_4 replacement is based on the ratio of CO_2 molecular diameter to cavity diameter of the sI hydrate structure, which is 1.0 for small cages and 0.834 for large cages, with CH_4 filling both small and large cages easily (Sloan Jr and Koh, 2007). As a result, CH_4-CO_2 replacement in small cages is exceedingly poor due to low permeability, and most CH_4 molecules remain in the small cages of sI hydrate. To increase the effectiveness of CO_2 injection and eliminate the difficulty of CO_2 injection at high pressures, a 77 percent N_2 and 23 percent CO_2 mixture was advised to inject into CH_4 hydrates (Schoderbek, Farrell, 2013, Kvamme, 2015). Large cages of sI hydrate are filled with primarily CO_2 during replacement processes in experimental experiments, while tiny cages are filled with N_2 (Merey, Al-Raoush, 2018, Xu, Cai, 2018).

STOMP-HYD takes into consideration mass and energy transfer in 3 mobile phases: aqueous, gaseous, and liquid CO_2, as well as 4 static phases: hydrate, ice, precipitated salt, and geologic medium (White and Oostrom, 2006, White, Wurstner, 2011). STOMP-HYD reveals that the higher permeability of the gas zone decreases CO_2 interaction with CH_4-hydrates to the boundary of the hydrate-bearing regions (White, Wurstner, 2011). Also, CO_2 injection at high pressure causes subsequent hydrate development and pore blockage (White, Wurstner, 2011).

MH-21 HYDRES is another commercial simulator that can be used to predict methane production from a class 1 methane hydrate reservoir (Kurihara, Ouchi, 2011, Kurihara, Ouchi, 2005, Masuda, Konno, 2008). MH-21 HYDRES can model three-dimensional (3D) Cartesian and two-dimensional (2-D) radial coordinates. Also, MH-21 HYDRES can distinguish six different components (methane, carbon dioxide, nitrogen, water, methanol, and salt), five phases (gas, water, ice, MH, and salt) during simulations. MH-21 HYDRES uses the Darcy equation to calculate permeability, gas, and water flows, and the Kim-Bishnoi equation to analyze MH dissociation kinetics as shown in Table 3 (Kim, Bishnoi, 1987). Under different conditions of depressurization, thermal stimulation, thermal flooding, inhibitor injection, nitrogen injection, and combinations technique, the MH-21 hydrate simulator can predict methane production (Narita, 2003).

Figure 5. depicts methane production from class 1-3 reservoirs using the MH-21 HYDRES model by depressurization, which takes into account saturation, absolute permeability, relative permeability, temperature, and bottom hole pressure (Konno, Masuda, 2010). Their findings demonstrate that increase in permeability led to an increase in CH_4 production when pressure is reduced. When other elements such as sediment characteristics remain constant, an increase in temperature boosts methane production in the reservoir due to an increase in flowability. The overall amount of output of gas from the class 1 methane hydrate deposit is approximately 240 million Sm^3 that is higher than class 2 and 3 methane hydrate deposits due to the free-gas zone below the MH zone and the gas-bearing MH zone (Konno, Masuda, 2010). It is followed by production from deposits of class 2 that contain hydrates and water zone, and class 3 which contains hydrate zone only as shown in Figure 3. For hydrate dissociation, only little changes in pressure and temperature are required and the presence of a free gas layer assurances methane production even when the hydrate dissociation is low (Moridis, Kowalsky, 2007, Xu and Li, 2015, Moridis, Collett, 2013).

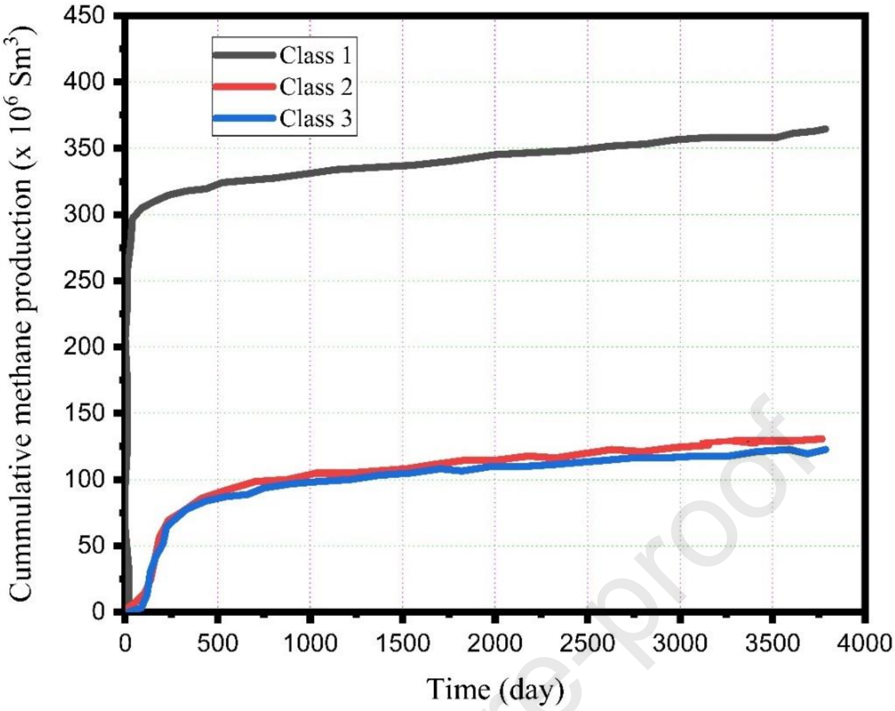

Figure 5. Cumulative CH_4 produced in MH deposit classes (**Konno, Masuda, 2010**).

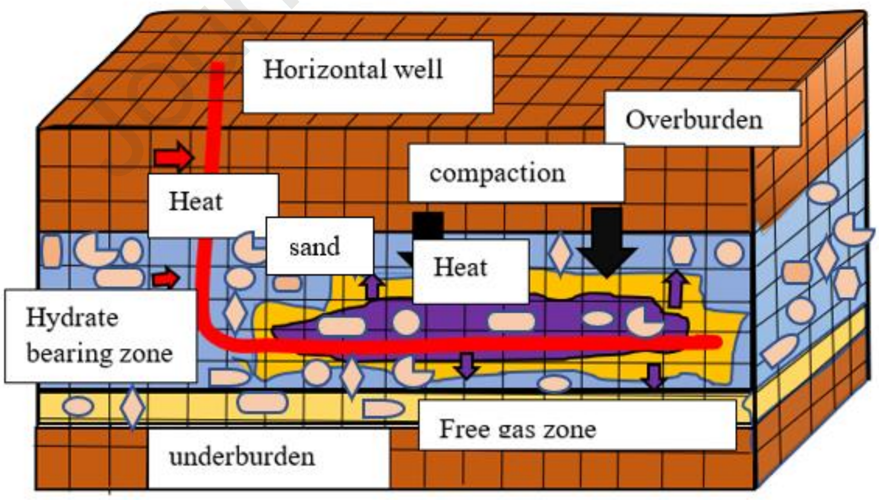

Figure 6. MH21-HYDRES (Kurihara, Ouchi, 2011).

(Kurihara, Sato, 2008, Kurihara, Ouchi, 2011) evaluated production methane by considering factors such as pressure, temperature, absolute permeability, effective permeability, porosity, MH saturation, water saturation, and clay content as observed in Figure 6. Results show gas output from Class 1 methane hydrate reservoir to be more than 70%, mostly contributed to the presence of free gas. Sparse distribution of the original MH in the reservoir was considered as a limiting factor to maximize its production Table 5. (Sasaki, Sugai, 2014) applied heating methods from a power plant and hot water, and an integrated thermal system, called 'Gas to Wire System, to predict gas production from methane hydrate (MH) during simulations. Parameters considered were well type, thickness, porosity, saturation, pressure, temperature, permeability. Their results of cumulative methane production for 15 years were 1.3 x 10^8 Sm^3. In the discussion above, all studies do not consider salinity factors that may affect the production of CH_4 from the Class 1 methane hydrate reservoir. The presence of gas hydrate can benefit from low salinity in this area because salt is an inhibitor of gas hydrate (Jenkins and Williams, 1984).

Table 4

Parameters and simulator in class 1 methane hydrate

Parameter	(Moridis and Kowalsky, 2006a)	(Konno, Masuda, 2010)	(Moridis, Kowalsky, 2007)	(Bai, Hou, 2020)	(White, Wurstner, 2011)	(Merey and Longinos, 2018a)
Porosity	0.3	0.4	0.3	0.35	0.3	0.5
Permeability (mD)	1000	500	1000	500	1000	1000
Initial pressure (kPa)	10670	6790	10670	7920	10670	23970
Initial temperature (°C)	13	(9 -14)	13.5	10.79	13.5	13.8

BHP (kPa)	4000	4000	4000	5000	4000	3000
Gas saturation	0.3	0.4	0.3	0.5		0.395
Hydrate saturation	0.7	0.6	0.7	0.5		0.37
Well radius		0.1				
salinity				0.015		0.0386
Simulator	TOUGH-Fx/HYDRATE	(MH21-HYDRES)	TOUGH-Fx/HYDRATE	CMG-stars	STOMP-HYD	HydrateResSim
Methods	depressurization	depressurization	depressurization	depressurization	Depressurization/ CO_2 injection	Depressurization/ CH4-CO2/N2 replacement

In all studies above none of the researchers have studied on comparison of these five simulators in Class 1 methane hydrate reservoir under different parameters shown in Table 4 well radius and salinity are not considered by all researchers. Hance no commonality between researchers on choosing parameters for the simulation. The different techniques discussed above could also be combined to evaluate their impact in recovering methane, however, this approach is not considered. Furthermore, research on methane hydrate production should concentrate on the use of dual wells to maximize production, increasing methane permeability in the reservoir to allow easy flow of methane in reservoirs, limiting the rise of the bottom well pressure to disrupt CH_4 equilibrium productions, and determining the critical surface area for methane hydrate dissociation kinetics.

Table 5

Simulators with maximum cumulative in class 1

Simulator	Parameter	methods	Effects	References
CMG STAR	porosity, permeability, pressure, temperature, saturation, wellbore, CO_2 injection rate, and well bottom hole pressure	Depressurization	The maximum cumulative 70%	(Walsh, Hancock, 2009, Uddin and Coombe, 2007, Llamedo, Provero, 2010, Uddin, Coombe, 2008, Sun, Ning, 2016)
TOUGH+HYDRATE	porosity, absolute permeability, Initial gas saturation, relative permeability, capillary pressure, thickness, gas production rate,	Depressurization	The maximum cumulative 75%	(Moridis, Kowalsky, 2007, Moridis and Kowalsky, 2006a, Alp, Parlaktuna, 2007)

	water saturation, and irreducible water saturation			
HydarteResSim	porosity, permeability, temperature, saturation, relative permeability capillary pressure, the thickness of hydrate, and thickness	Thermal, with total heat of 5400 J/s was applied, at a pressure of 2700 kPa for 8.4 years	The maximum cumulative is 52 %.	(Merey and Sinayuc, 2016)
STOMP-HYD	permeabilities, capillary pressure, porosity, liquid CO_2 effective saturation, Gas effective saturation, and aqueous effective saturation	depressurization CO_2 injection	Add 10% cumulative after depressurization	(White, Wurstner, 2011)

MH-21 HYDRES	pressure, temperature, absolute permeability, effective permeability, porosity, well type, thickness saturation, and clay content	Depressurization	The maximum cumulative is 74.8%	(Kurihara, Sato, 2008)

3.2 Simulating methane production from class 2 methane hydrate reservoirs

Class 2 gas hydrates are the most problematic targets for methane production due to their poor permeability and thermal characteristics. Therefore, depressurization and thermal combination techniques are the current mechanisms for recovering gas hydrates from class 2 methane hydrate reservoirs (Moridis, 2004a). High hydrate saturation, heat, and limited permeability are common in Class 2 gas hydrates. Increasing the permeability of the reservoirs via enhancing fracking enhances the flow of gas in the reservoirs (Moridis, 2004a). With the increase in the amount of heat available for dissociation, gas release in the reservoir increases with the relative heat of the injected water in class 2 (Moridis, 2004a). Reagan (Reagan, 2009) utilized T+H to simulate methane production from a Class 2 methane hydrate reservoir. In hydrate formation and dissociation, it combines an equilibrium and a kinetic model. (Moridis and Kowalsky, 2006b) simulated Class 2 methane hydrate gas output with a solid aquifer and suggested that for successful gas production from gas hydrate reservoirs depressurization process is not suitable. The combination methods (depressurization and thermal) showed that production rate and efficiency strongly lead to a higher production over a short period depend on formation porosity, formation anisotropy, and short well spacing (Moridis and Reagan, 2011) considered Hydrate zone thickness, pressure, temperature, gas, and hydrate phase saturations (SG and SH), thermal conductivity, Relative permeability, Intrinsic permeability to predict methane gas through (T+H) simulator. They observed a large volume yield of gas at high rates over the entire production period, which was in parallel with the decline of water production. "Original Porous Medium" (OPM) model was used with the following common assumption 1) The development of hydrates does not affect the medium porosity), 2) During the production of solid phases, the intrinsic permeability of the porous media does not alter and 3) The increase of relative permeability improves production, 4) The fluid flow is regulated by the saturation of the different phases in the pores. During the 2400 to 5860 days of production, gas yield rapidly increased first due to depressurization, then became constant that was followed by a slow decline mostly contributed by pressure reduction in the reservoir that affected gas dissociation. The use of horizontal wells will significantly increase the output of gas from these sources' deposits.

(Xia, Hou, 2017) used a combination of depressurization and heating approaches to investigate CH_4 production from class 1, 2, and 3 hydrate reservoirs. Bottom-hole pressure, reservoir temperature, hydrate saturation, intrinsic permeability, and heating power were all taken into account. Figure 7 show that the CH_4 production rate for a class 1 methane hydrate reservoir is high early in the production time when the majority of the CH_4 is produced; for a class 2 methane hydrate reservoir, the CH_4 production rate is high throughout the entire production period; and for a Class 3 methane hydrate reservoir, the CH_4 production rate varies periodically. During three production years, class 1 recovery efficiency was 49.1% but assisted by 31.3 percent, class 2 recovery efficiency was 72.4 percent but enabled by 74.6 percent, and class 3 recovery efficiency was 7.7% but aided by 8.3 percent methane hydrate dissociation as indicated in Figure 7.

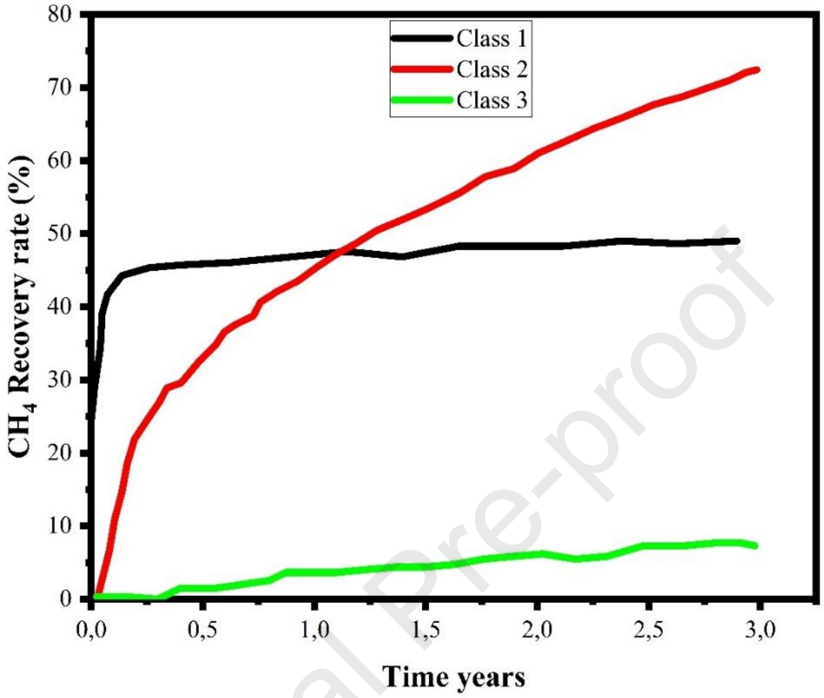

Figure 7. CH_4 recovery % of the methane hydrate reservoirs (Xia, Hou, 2017).

Furthermore, another alternative method like CO_2 injection is recommended for future studies to evaluate its potential to recover methane from class 2 methane hydrate reservoirs. CO_2 is stabler than CH_4 hydrate in a particular temperature and pressure range only (Jemai, Kvamme, 2014). The most stable hydrate would fill CO_2 into most of the major holes while CH_4 takes up small spaces until CO_2 is no longer present in the end, at which point CH_4 hydrate is formed. CO_2 has a molecular weight of 44 grams, which is higher than the 16 grams of CH_4, and a kinetic diameter of 0.33 nanometers, which is smaller than the 0.38 nanometers of CH_4 (Li, Falconer, 2004). CO_2 is heavier and has a smaller kinetic diameter than CH_4, resulting in a quicker diffusion rate in reservoirs and the ability to be competitively adsorbed into (tiny) pores due to its higher adsorption affinity (McGrail, Zhu, 2004, Cui, Bustin, 2004, McGrail, Schaef, 2007). Also, the study by (Busch and Gensterblum, 2011, Ruthven, 2008) reveals that CO_2 has greater sorption than methane and water, thus its injection can facilitate methane displacement from class 2 methane hydrate reservoirs through chemisorption and physisorption.

Furthermore, while CO_2 is thermodynamically preferable to CH_4 in CH_4-hydrate, the heat generated by the formation of CO_2-hydrate is 20% higher than that required to dissociate CH_4-hydrate, and it is assumed that the mechanical stability of the hydrate-bearing formations will be maintained during the development by refilling pore space with CO_2-hydrate. Also, studies though in shale gas indicate essential factors that control CH_4 recovery and CO_2 storage, reservoir pressure gradient, competitive adsorption, flow dynamics, and shale properties were established (Iddphonce, Wang, 2020) could be replicated in the study of the contribution of CO_2-CH_4 competitive during the production of methane hydrate.

Furthermore, methane production from class 2 methane hydrate reservoirs can be simulated by using STARS, whereas, changes in injection pressure, temperature, reservoir properties, hydrate blocking models, intrinsic kinetic rates for CO_2 hydrate formation, and numerical parameters are considered to perform sensitivity analysis on CH_4 output. Huneker (Huneker, 2010) applied STARS simulation and found that CO_2 injection increases CH_4 production by 50-60 % (through hydrate dissociation and depressurization) when reservoir temperature is in the range of 1.4 ^oC – 18 ^oC. (Li, Li, 2021) considered porosity, intrinsic permeability, pressure, temperature, saturation, layer thickness, and bottom-water volume to simulate methane production of class 2 methane hydrate through depressurization and heat transfer mechanisms. In this model, the total gas recovery in 2000 days was about 87.8 %. (Sun, Xin, 2016) observed that perforation intervals, bottom hole pressure, and well spacing are the key factors to be considered in the prediction of methane production from the class 2 reservoir. (Liu, Bai, 2018) illustrate that the higher reservoir conductivity leads to more gas output during the depressurization process, but less in the hot water flooding process due to lower remaining natural gas hydrates reserves and bottom water coning.

Despite promising predictions, STARS is only capable of using kinetic equations and cannot integrate equilibrium line changes. Also, no researchers suggest the use of the CO_2 swapping technique in a CMG STAR simulator using a horizontal well to recover methane from Class 2 methane hydrate. CO_2 swamping has additional benefits of CO_2 sequestration that may improve methane production and formation stability.

On the other hand, the use of HydarteResSim (HRS) in class 2 methane hydrate reservoirs is reviewed with various scholars. (Sridhara, Anderson, 2018) used CO_2 injection to improve methane recovery from Class 2 hydrate by considering some petrophysical parameters: saturation, porosity, pressure, temperature, intrinsic permeability, initial effective permeability, thermal conductivity, pore compressibility, rock specific heat, and rock grain density. Their results of cumulative methane volume production for 15 years were $2.25 \, x \, 10^7 \, m^3$ and for CO_2 $2.75 \, x \, 10^7 \, m^3$ as indicated in Figure 8. HydarteResSim simulation involves three steps that are vertical well, which serves in the first step as an injector, and the third step as a maker, while the intermediate step is for harmonization. CO_2 is first pumped into the underlying aquifer, followed by the well shut down to allow injected carbon dioxide gas to transform into CO_2 - hydrate. During the depressurization process (third step) CH_4 hydrate is decomposed, facilitating gas and water production. Over 15 years of operation, results show that a rise in temperature ranges from 5.0 °C to 7.5 °C represents the theoretical (adiabatic) shift in recovery from 4.4 % to 10.0 %.

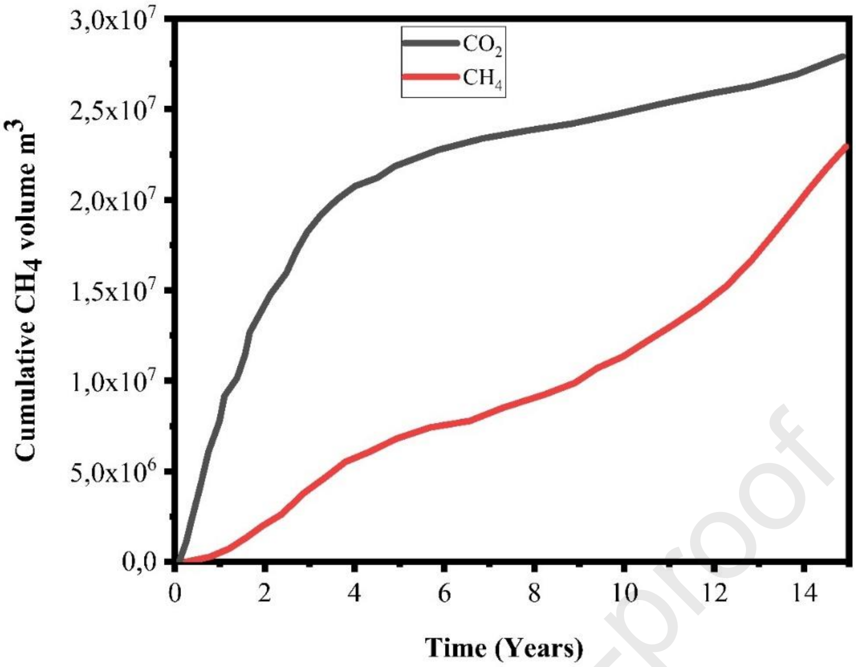

Figure 8. Cumulative volumes of CH_4 and CO_2 form class 2 methane hydrate (*Sridhara, Anderson, 2018*)

MH-21 HYDRES is another simulator utilized for predicting methane production from a class 2 methane hydrate reservoir. (Kurihara, Funatsu, 2008) considered pressure, temperature, saturation, and permeability on the prediction of methane production to evaluate methane recovery from Mallik gas hydrates reservoir. Results show that the cumulative output of gas and water over the entire test period is estimated at 830 m^3 and 20 m^3, respectively. During testing, the presence of sand in the reservoir was observed to improve permeability that significantly increased gas production rates. (Khetan, Das, 2013) applied MH-21 HYDRES simulations to predict the production of methane through depressurization and CO_2 injection techniques. They considered the Darcian theory, multiphase, unstable, non-isothermal, and kinetic model that incorporates mass, momentum, and energy conservation in a porous reservoir. The results confirm a rise in the rate of methane recovery due to CO_2 injection, which is primarily due to the displacement of CH_4 by CO_2. Table 7 shows the percent of CH_4

generation from several simulators in class 2 methane hydrate reservoirs using various production strategies.

Table 6

Parameters and simulator in class 2 methane hydrate

Parameter	(Moridis, 2004a)	(Xia, Hou, 2017)	(Moridis and Reagan, 2011)	(Li, Li, 2021)	(Sridhara, Anderson, 2018)
Porosity	0.28	0.35	0.35	0.21	0.35
Permeability (mD)	20 - 1000	1000		1000	10
Initial pressure (kPa)	10000	10670	10670	9000	6494
Initial temperature (°C)	7.5	13.3	13.3	7.55	4.48
BHP (kPa)	9000 - 10270	3000	12240	4000	3500
Water saturation	0.2	0.3	0.3	0.5	0.3
Hydrate saturation	08	0.7	0.7	0.5	0.7
salinity		0.015	0.035		0
Simulator	TOUGH2 family	HydrateResSim	TOUGH+ HYDRATE	CMG-STARS	HydrateResSim
Methods	Depressurization/ thermal	Depressurization/ thermal	Depressurization/ thermal	depressurization	CO2 swamping/ depressurization

Despite the consideration of several parameters as discussed for class 2 gas hydrates, future studies are recommended to account for reservoir fracking before methane production to improve reservoir permeability. In addition, Table 6, shows differences in methane generation that can be attributed to differences in permeability, BHP, initial pressure, and temperature in between researchers. Although many researchers employed combination methods (depressurization/thermal or CO_2 swamping/depressurization) in this class and had good results. Geomechanical stability is important because it influences vertical displacement "down" (subsidence) at the reservoir's center or top, as well as sea bed stability. Increasing reservoir pressure has an impact on methane gas output (CMG, 2017). The salinity should be observed in the reservoir because it can affect inhibitors when combining with depressurization techniques due to the formation of precipitation that hinders the permeability of gas (Moridis and Reagan, 2007). Furthermore, additional enhancement studies on control sand generation and rehydrate development during methane production from methane hydrates should be conducted.

Table 7

Simulators with maximum cumulative in class 2

Simulator	Parameter	methods	Effects	References
CMG STAR	porosity, permeability, pressure, temperature, saturation, wellbore, CO_2 injection rate, and well bottom hole pressure	Depressurization and thermal Depressurization & CO_2 swapping	The maximum cumulative is 87.8% The maximum cumulative is 72.4%	(Xia, Hou, 2017, Li, Li, 2021)
TOUGH+HYDRATE	porosity, absolute permeability, initial hydrate saturation, relative permeability,	Thermal depressurization	The maximum cumulative is 49.06%, 61.99%,	(Song, Cheng, 2015)

	capillary pressure, thickness, gas production rate	Combination method	74.87%	
HydarteResSim	porosity, permeability, temperature, saturation, relative permeability capillary pressure, the thickness of hydrate, and thickness	Depressurization	The maximum cumulative is 10.0%.	(Sridhara, Anderson, 2018)
MH-21 HYDRES	pressure, temperature, absolute permeability, effective permeability, porosity, well type, thickness saturation, and clay content	Depressurization	The maximum cumulative is over 36%	(Kurihara, Sato, 2008, Kurihara, Ouchi, 2011)

567

3.3 Simulating methane production from class 3 methane hydrate reservoirs

Owing to the high saturation of the hydrate, flow in class 3 is unlikely without fracturing due to low fracture permeability that poses production challenges. The method of depressurization is the most achievable and efficient related to other methods. Increasing hydrate temperature is a determinant factor that affects the stability of a given pressure and intrinsic permeability, and enhances gas production. The depressurization method is only capable of producing 7 -36 % of the total gas in place, and this has led previous studies to the conclusion that Class 3 deposits have low potential and are therefore un-economical targets for development (Konno, Masuda, 2010, Moridis, 2004a, Xia, Hou, 2017, Moridis, Collett, 2004). Fracturing increase the permeability that enhances gas dissociation which collectively improves methane production due to the following factors; (i) The increased surface area exposed to hot water, and (ii) the Increase gas release pathway system (Moridis, Collett, 2005). The rate of CH_4 generation is determined by saturation. Lower saturations result in a higher production rate due to a bigger effective initial permeability to water and, as a result, faster depressurization and hydrate dissociation. As a result, when SH0 = 0.5, the production rate is higher than when SH0 = 0.7, and it is highest when SH0 = 0.3 in the early phases of production (Moridis and Reagan, 2007). On the other hand, (Li, Moridis, 2011) investigated the impact of the fracking process through the use of injected brine in a huff and puff process facilitated by depressurization and thermal mechanisms. Production was found to depend on the length of huff and puff, the temperature of brine, and the rate of production.

(Chen, Feng, 2018b) utilized a multi-layer model with the following assumptions, utilized (T + H) to forecast methane production (1) Darcy's Law and the capillary effect were used to investigate multi-phase flow. (2) The methane hydrate is stationary, (3) Permeability changes with porosity, (4) The bearing layer does not reform, and (5) The kinetic dissociation model follows Kim's law (Kim, Bishnoi, 1987, Clarke and Bishnoi, 2001a, Clarke and Bishnoi, 2001b). The following parameters were considered: Hydrate layer height, hydrate saturation (SH), porosity, permeability, pressure, temperature, gas saturation in class 3 methane hydrate reservoir to estimate methane production from Class 3 methane hydrate reservoir (Chen, Feng, 2018b, Chen, Yamada, 2016, Chen, Yamada, 2017, Jin, Xu, 2016). Their findings show that the output increases considerably with the rise of the initial reservoir temperature. Hydraulic fracturing boosts methane output via increasing fracture permeability, well spacing, hydrate exploitation, and the enhancement effect (Chen, Feng, 2018b, Chen, Yamada, 2016, Chen, Yamada, 2017, Jin, Xu, 2016). Figure 9 shows the rate and cumulative production of CH_4 and H_2O in reservoirs with no fractures and with fractures were observed as 61.6%, to 80.6%, and the recovery ratio increased as fracture permeability increased (Zhong, Pan, 2020).

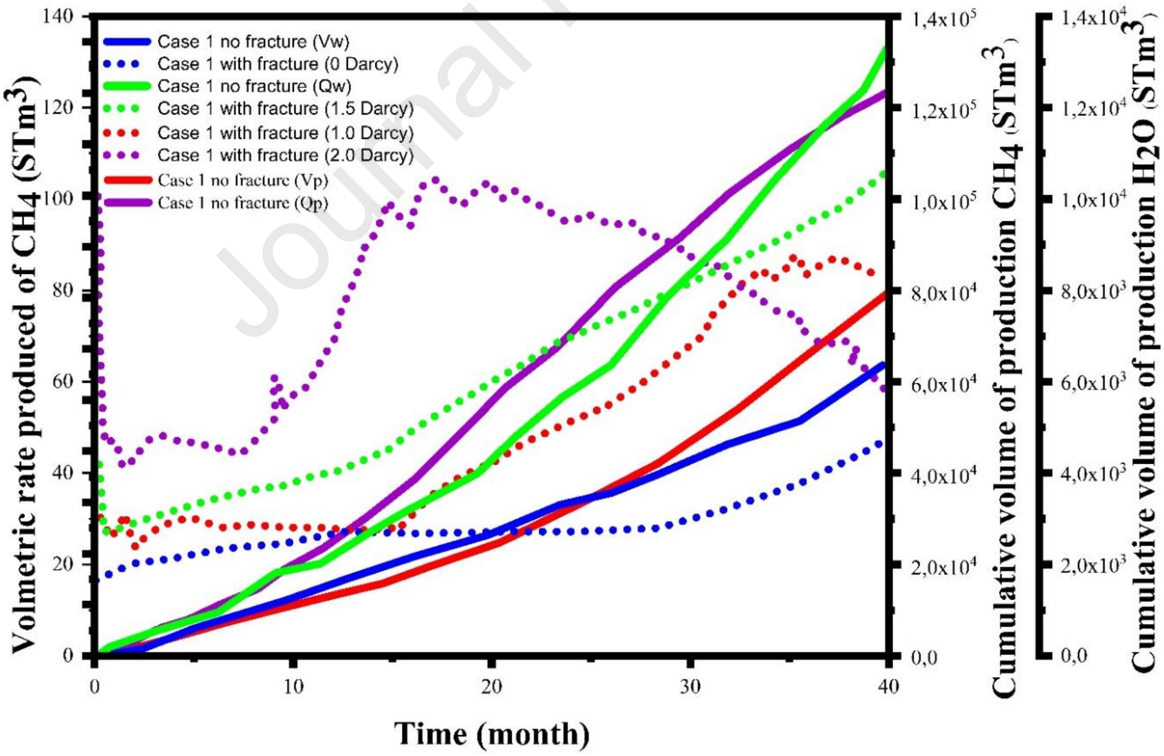

Figure 9. Production of CH_4 and H_2O in fracture with different permeability modified from (Zhong, Pan, 2020).

Furthermore, the use of a combination of depressurization and thermal techniques reveals that CH_4 production performance is influenced by the hydrate deposits' intrinsic permeability, the porosity of the sediments, the rate of injection and output, the temperature of the injected water, and the water's irreducible saturation (Moridis and Reagan, 2007, Li, Li, 2012, Moridis, Kim, 2013). Furthermore, findings show that when initial reservoir temperature and permeability increase by a similar factor, the cumulative output increases by one order (Chen, Feng, 2018b). However, permeability and porosity show that: 1) the heterogeneity of the hydrate stability zone affects the movement of methane within it and affects the formation and deposition of hydrate, 2) in a heterogeneous layered reservoir, there are stratified variances in gas lateral migration, hydrate formation in the sediment, and the horizontal distribution range of the sediment (Bei, Xu, 2019).

The combination of depressurization and thermal, or depressurization and CO_2 injection methods under consideration of the geomechanical process is highly recommended in future studies. Also, evaluation of the effects on methane recovery of factors like well type, well spacing, bottom hole pressure, and perforation intervals should be assessed to analyze how they affect methane production in class 3 methane hydrate reservoir.

(Zatsepina, Pooladi-Darvish, 2011) used STARS in the prediction of CH_4 production from class 3 methane hydrate reservoir by considering the following factors: Porosity, permeability, saturation, pressure, temperature. Results show that the recovery factor is 35% in 7.5 years facilitated by equilibrium reaction and depressurization mostly affected by permeability, Heat, and fluid flow. Finding from (Huang, Wu, 2016) indicated that when the pressure drops by 70%, the recovery factors for a 20-year operating period are 0.37, 0.47, 0.49, 0.51, and 0.13 for initial hydrate saturation of 30%, 40%, 50%, 60%, and 70% respectively. The low permeability limits the amount of decomposing hydrates due to the reduction in pressure, affecting the heat transfer surface area.

Furthermore, (Yang, Lang, 2014) adopted HydrateResSim to study methane production from Shenhu site SH7 in China through depressurization and thermal methods in a horizontal drilled well. Results show that at 42 ° C well temperature and 1.383 x 10^6 Pa, 2.766 x 106 Pa well strain pressure, more than 20% of hydrates in reservoirs are dissociated within 450 days. Similarly, (Merey and Sinayuc, 2017) applied HydrateResSim, considering three assumptions as proposed by (Moridis, Kowalsky, 2005b) in porous media, the Darcy law is valid, the geological medium is stable, porosity variation is a pressure and temperature phenomenon, and output takes place when pressure is below 10000 kPa. Factors such as intrinsic permeability, temperature, pressure aqueous saturation, hydrate saturation, and gas saturation were considered in the simulations. Gas recovery was performed through the depressurization process. According to (Merey and Longinos, 2018b) once the pressure is lower leads to more methane production. However, the use of the depressurization process will lead to the formation of ice (due to the endothermic nature of the dissociation of gas hydrates) and the production of sand that can affect the production of gas (Merey and Sinayuc, 2016, Uchida, Klar, 2016).

HydrateResSim shows that the Class 1 hydrate reservoir has a high rate of methane production in the initial time due to the free gas layer. Whereby the Class 2 methane hydrate deposit, the rate of methane production remains maximum during the entire production era, while for the Class 3 methane hydrate reservoir, the rate of methane production has varied regularly (Merey and Longinos, 2018a, Xia, Hou, 2017). Despite these predictions, HydrateResSim lacks geomechanical codes, and so does not evaluate the geomechanical effects during methane gas production (Merey and Longinos, 2018a).

MH-21 HYDRES is another simulator that is utilized to estimate gas recovery from methane hydrate reservoirs. (Anderson, Kurihara, 2011) assessed class 3 methane hydrate reservoir from Mount Elbert using MH-21 HYDRES. In the simulations, they considered parameters such as reservoir thickness, porosity, hydrate saturation, intrinsic permeability, the salinity of pore water, intrinsic permeability, bottom-hole pressure, and temperature. Over 50-year of operation, the methane gas production rate continued to increase to the maximum rate of about 10,000 Sm^3/day due to depressurization that enhanced methane dissociation. Initial reservoir temperature, intrinsic reservoir permeability, and relative permeability in the presence of hydrate, as shown in Figure 8, are the most critical parameters affected by gas production. (Kurihara, Ouchi, 2011) predicted methane production through MH-21 HYDRES with production efficiencies showing 30 to 60%, assuming depressurization is applied for 8 years with a bottom hole pressure of 3000 kPa. The total amount of CH_4 generated in the horizontal well over the first ten years and the subsequent twenty years is 2.65 x 10^6 and 2.41 x 10^6 ST m^3, respectively, with average methane production rates of 0.74 x 10^3 and 0.38 x 10^3 ST m^3/day, which are both less than 0.3 percent of the rule-of-thumb for commercially viable gas well production rates (3.0 x 10^5 ST m^3/day). (Li, Yang, 2012) show the results of the cumulative amount of methane produced in the horizontal well throughout of 1^{st} 10 years then 20 years later are 2.65 x 10^6 and 2.41 x 10^6 ST m^3 by the consistent average methane gas production rates of 0.74 x 10^3 and 0.38 x 10^3 ST m^3/day, respectively, that are less than 0.3% of the rule-of-thumb which are (3.0 x 10^5 ST m^3/day) for commercially gas well production rates.

Collectively, compared to all simulators (discussed), CMG STARS and TOUGH + HYDRATE have a higher prediction for methane production (Figure 10) and Table 9. To reflect the production efficiency of CMG STARS hydrate deposition in porous media, several researchers have validated its accuracy and suitability (Uddin, Coombe, 2008, Uddin, Wright, 2011, Hong, Pooladi-Darvish, 2003). HydrateResSim has a limitation of not predicting geomechanical changes with distinct production methods during gas production, it assumes that sediments are stationary (Merey and Longinos, 2018a). TOUGH + HYDRATE, On the other side, it involves both equilibrium hydrate formation and dissociation, as well as a kinetic model for heat and 4 mass components (gas, water, hydrate, and inhibitor) divided into 4 phases (gas, liquid, hydrate, and ice phases) (Yu, Guan, 2020). Their result shows that apart from depressurization, thermal injections increase production by 31.9% in 20 years. Both lab and field test data have validated the efficiency of this simulator (Chen, Feng, 2018a, Chen, Feng, 2018b, Sun, Ning, 2016, Li, Li, 2014a, Li, Li, 2014b, Li, Li, 2014c, Feng, Chen, 2019, Yu, Guan, 2019a, Yu, Guan, 2019b, Sun, Ma, 2019).

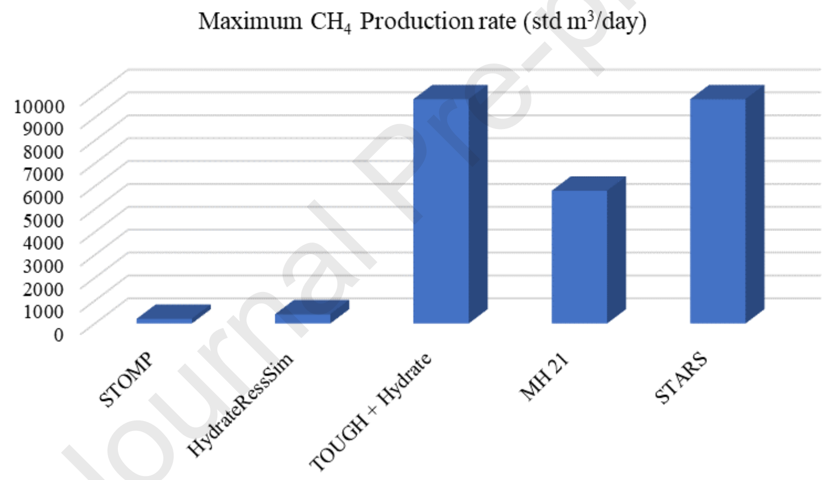

Figure 10. Maximum gas production from class 3 methane hydrate reservoir as predicted by simulators (Anderson, Kurihara, 2011).

In view of the discussed methods for producing methane from class 3 gas hydrate reservoirs, a lack of common understanding exists among scholars particularly on which process is suitable for methane production. Many parameters were investigated with many scientists like porosity, absolute permeability, Initial gas saturation, relative permeability, capillary pressure, thickness, gas production rate, water saturation, and irreducible water saturation. In various studies, absolute permeability, BHP, the thermal conductivity of the rock, porosity, sediment particle density, and surface area were the parameters that showed the most recovery of methane from gas hydrates (Giraldo, Klump, 2014).

Table 8

Parameter	(Merey and Longinos, 2018a)	(Xia, Hou, 2017, Li, Li, 2012)	(Zatsepina, Pooladi - Darvish , 2011)	(Yang, Lang, 2014)	(Sun, Xin, 2016)	(Vishal, Lall, 2020)
Porosity	0.5	0.3	0.3	0.41	0.083	0.5
Permeability (mD)	1000	1	1000	75	17.73	100
Initial pressure (kPa)	24180	2930	10000	13830	1000	29000
Initial temperature (°C)	13.8	1	12	14.15	10	4
Well spacing (m)					1000	
BHP (kPa)	3000	400	2800	1000	3000	
Water saturation		0.6	0.3	0.56		
Hydrate saturation	0.374	0.4	0.7	0.44		0.5
Perforated intervals					13	
Well type					Vertical	
Simulator	HydrateResSim	TOUGH + HYDRATE	CMG Star	HydrateResSim	CMG Star	TOUGH + HYDRATE
Methods	Depressurization/ CH_4-CO_2/N_2 replacement	depressurization and thermal	depressurization and thermal	depressurization and thermal	depressurization and thermal	depressurization and thermal

Parameters and simulator in class 3 methane hydrate

As can be observed in Table 8, there was no consensus among the researchers on the parameters to use, for example, perforated intervals, well spacing, and well type, which some scholars did not consider in simulation. Furthermore, the scarcity of knowledge for several simulators in class 3 necessitates additional research for example (STOMP-HYD). In addition, the conditions applied to produce methane from the identified methods are not clearly explained, and literature on the identified methods is scarce. Furthermore, more research is needed on the combination of depressurization and CO_2 injection using a dual well and horizontal well to boost methane output while also storing CO_2.

Table 9

Simulators with maximum cumulative in class 3

Simulator	Parameter	methods	Effects	References
CMG STAR	Porosity, permeability, saturation, pressure, temperature	Depressurization,	The maximum cumulative is 35%	(Zatsepina, Pooladi-Darvish, 2011)
TOUGH+HYDRATE	porosity, absolute permeability, Initial gas saturation, relative permeability, capillary pressure, thickness, gas production rate, water saturation, and irreducible water saturation	Depressurization, Thermal, and hydraulic fracturing	Ranges of maximum cumulative in a reservoir that has no fracture and which have the fracture were 61.6%, to 80.6%,	(Zhong, Pan, 2020)

HydarteResSim	porosity, permeability, temperature, saturation, relative permeability capillary pressure, the thickness of hydrate, and horizontal well	Depressurization, Thermal	The maximum cumulative is more than 65 %.	(Yang, Lang, 2014)
MH-21 HYDRES	pressure, temperature, absolute permeability, effective permeability, porosity, well type, thickness saturation, and clay content	Depressurization	The maximum cumulative is 60%,	(Kurihara, Ouchi, 2011)

710

4. Field case production

There is scarce literature on-field methane production from methane hydrate reservoirs leading to limited information on the real experience encountered during production shown in Table 10.

4.1 Messoyakha

The Messoyakha gas field with 24 x 10^9 m^3 methane hydrates in place. December 1969 started a field test trail; 57 wells were drilled. The depressurization methods, thermal techniques, and inhibitors such as calcium chloride and methanol were used to produce methane from methane hydrate (Makogon and Omelchenko, 2013). However, the pressure and local temperature fluctuations caused the gas hydrates to self-preserve. Messoyakha is a class 1 methane hydrates reservoir with contains sandstone, interbed shale, porosity 0.16 to 0.38 and a mean of 0.25, initial temperature T = 8 to 12°C mean 10°C, irreducible water saturation 0.29 to 0.50 with a mean value of 0.40, hydrate saturation 0.20, gas saturation 0.4, permeability 203 mD, perforation interval 16m, preliminary reservoir pressure 7700 kPa reduced to 3039.75, and water salinity not exceeding 0.015 (Makogon and Omelchenko, 2013, Collett and Ginsburg, 1998). To check the presence of CH_4 – hydrate, an inhibitor method was used (Makogon and Omelchenko, 2013). The bottom hole temperature increase caused by mixing water and methanol will be reported as negative enthalpy when methanol is injected into the aquifer. Until 2011, 4 wells and 10 control wells operated through an average production rate of 1.8 x 10^4 to 9.8 x 10^4 m^3 /day and Messoyakha was the only gas hydrate field that produces methane for commercial (Makogon and Omelchenko, 2013). Figure 10. Show the total amount of CH_4 released by this reservoir as 12.9 x 10^9 m^3. Since the total volume of water generated is 48 x 10^3 m^3, a water-saturated layer occurs between the free CH_4 and hydrate zones.

The method adopted in this field test is compared with the approach applied in the simulation studies as reported by (Moridis, Kowalsky, 2007, Grover, Holditch, 2008, Moridis and Kowalsky, 2006a, Alp, Parlaktuna, 2007, Zhu, Xu, 2020) TOUGH+HYDRATE (Grover, Holditch, 2008) using depressurization methods, considered various parameters like permeability, reducing pressure, porosity, saturation, perforation interval, and temperature change. The effective gas permeability control dissociation of the gas hydrate by controlling pressure in the reservoir. Also, water drive in a hydrate-capped gas reservoir does not aid in the production of gas from hydrates but rather clogs the perforations (Grover, Holditch, 2008, Moridis and Kowalsky, 2006a) Figure 11. The amount of water collected from hydrate dissociation is considerably greater than that obtained from wells, water obtained from hydrate dissociation remains in the reservoir, leading to increase pressure relief that cannot be overlooked.

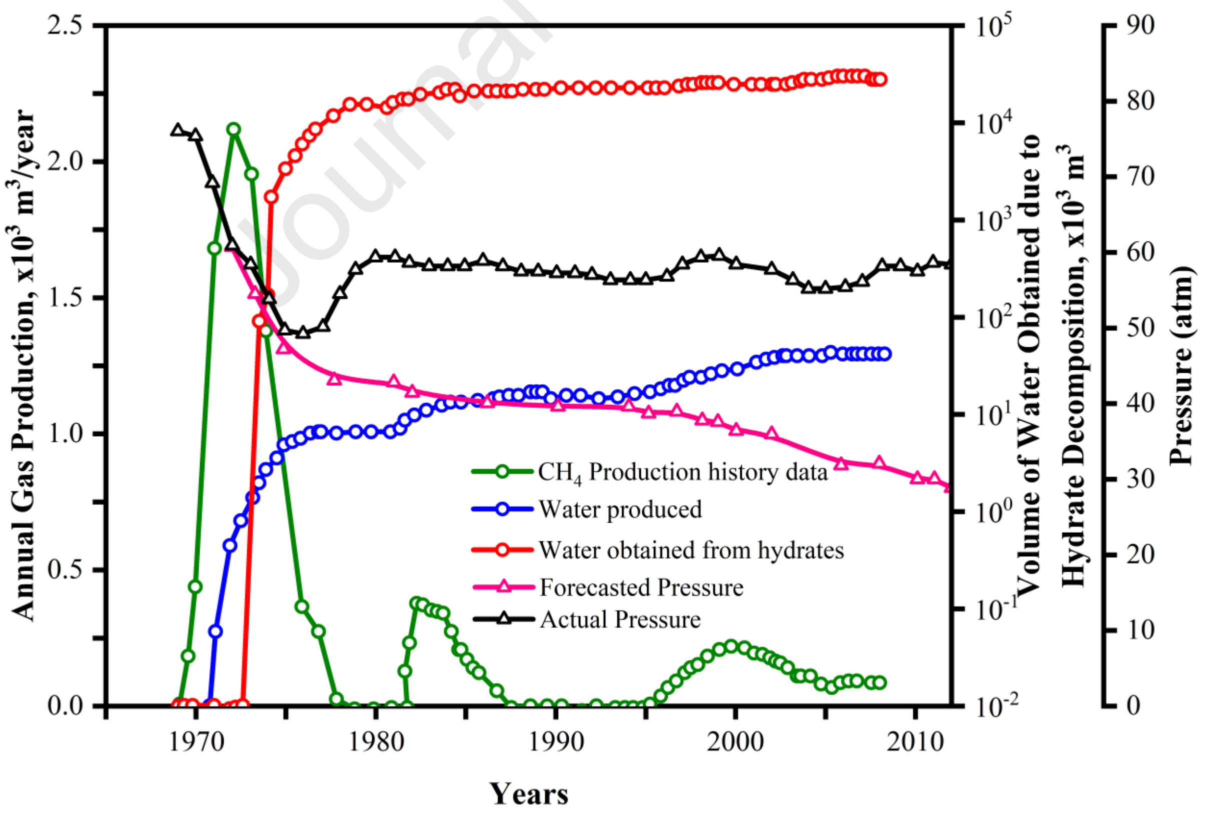

Figure 11. Cumulative H_20 intrusion into the formation and H_2O produced from the deposit (Makogon and Omelchenko, 2013)

Also, Figure 12 represents the real pressure actions versus the model's pressure. The values estimated with the model closely followed the real data, as shown in Figure 12. with the largest deviation of 5percent. The isothermal model pressure support through water and gas injection at a constant temperature (for this case 10 ^{o}C was used and pressure reduced from 9000 kPa to 5500 kPa). While non-isothermal simulations take up more CPU time than isothermal simulations. In addition, the initial temperature was 9.8 degrees Celsius, which dropped due to the Joule-Thomson effect and hydrate breakdown around the wellbores. Therefore, in non-isothermal, the temperature changes in field development are not constant like in isothermal. Figure 13 shows the real pressure actions versus the pressure obtained with the experiment, as well as the model's output rates versus the actual production rates. Except when the decomposition process was started, the change in values does not exceed five percent. The inaccuracy of the decomposition kinetic model is most likely to blame for this deviation.

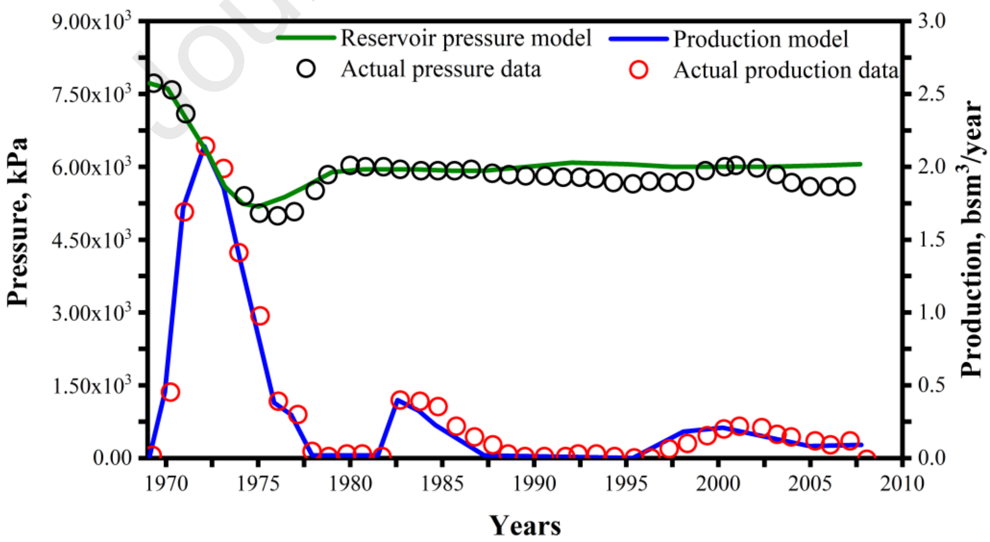

Figure 12. Record related with pressure in the isothermal model

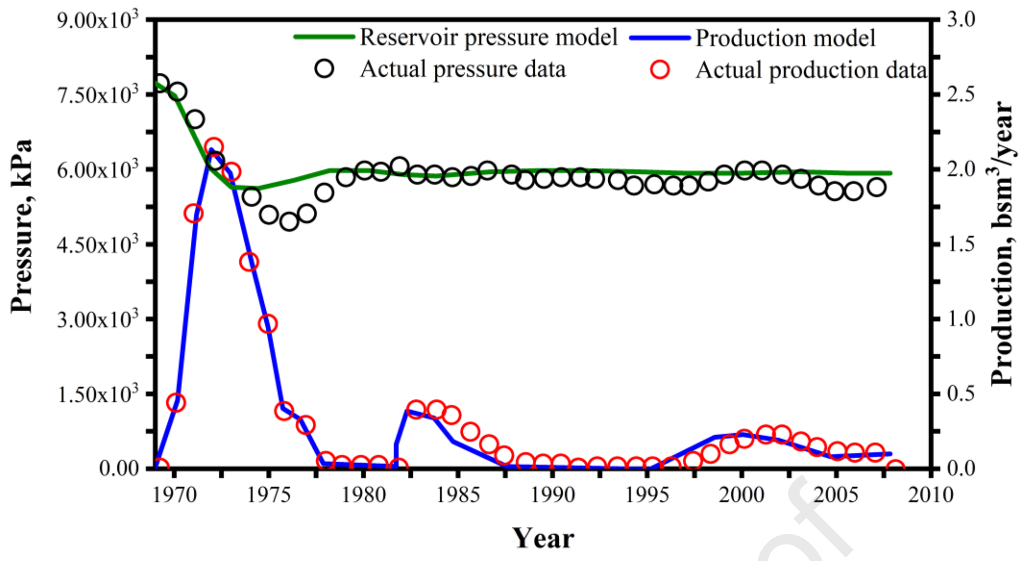

Figure 13. Outcomes numerically from the nonisothermal

Figure 14 depicts the change in temperature in the region. The mean equilibrium temperature for the Messoyakha is about 10^0C. The field's reservoir pressure was constant, but it varies by environment atmospheres, possibly due to the influence of gas hydrate self-preservation. During output from Class 1 deposits, wellbore heating is needed to prevent secondary hydrate formation, which can limit flow and eventually choke the well.

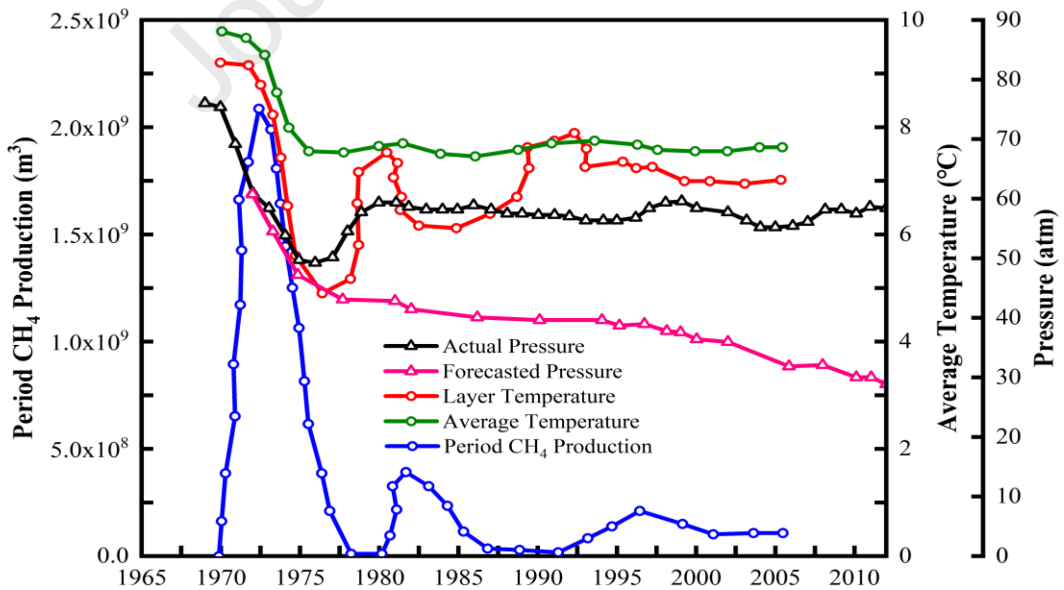

A

Figure 14. Output was found in the STARS simulator modified from (Makogon and Omelchenko, 2013).

4.2 Mallik

In December 2007, (Kurihara, Sato, 2010) reported field test case production from the Mallik 2007 field in Canada, using a depressurization method to create gas by reducing the pressure in the bottom hole from 11000 kPa to 7000 kPa in the perforated interval of 12 m. parameter of the reservoir was lithology of shaly sandstone, porosity 10 – 40, methane hydrate saturation 0.5 – 0.95, water saturation 0.5 – 0.05, absolute permeability 100 -1000 mD, effective permeability of water 0.001 to 1 mD, initial pressure 11100 kPa, and initial temperature 12^0C. During the 60 hours of operation, production only lasted for 30 hours. Produced methane failed to reach the surface as it accumulated at the top of the casing and affected production. In addition, produced water flowed into the aquifer instead of flowing to the surface. There is no clear information on how much gas and water were produced in this test. The test resumed in 2008 employing depressurization, by lowering the pressure in the bottom hole to about 4500 kPa, sand screening, and heating methods, however, production succeeded by using depressurization and thermal but lasted for 6 days. Figure 15 indicates Step 1 when pressure is reduced from 11000 to 6800 kPa production for CH_4 is 4700 m^3, average rate 2300 m^3/day and for water 20 m^3, average 9.5m^3/day. Step 2 when pressure reduced from 6800 to 5200 kPa production for CH_4 5100 m^3, average rate 1900 m^3/day and for water 30 m^3, average 11.2 m^3/day. Step 3 when pressure reduced from 5200 to 4200 kPa production for CH_4 3100 m^3, average rate 2600 m^3/day and for water 18 m^3, average 15.5 m^3/day. Also, due to the rapid decline of methane production (4000 m^3/day -1500 m^3/day). on the other hand, water produced ranged from 30 to 40 m^3/day (Kurihara, Sato, 2010). Stable production of methane varied from 2000-3000 m^3/day while water production was from 10-20 m^3/day indicating the potential of the reservoir's CH_4 and H_2O production (Makogon and Omelchenko, 2013, Kurihara, Sato, 2010).

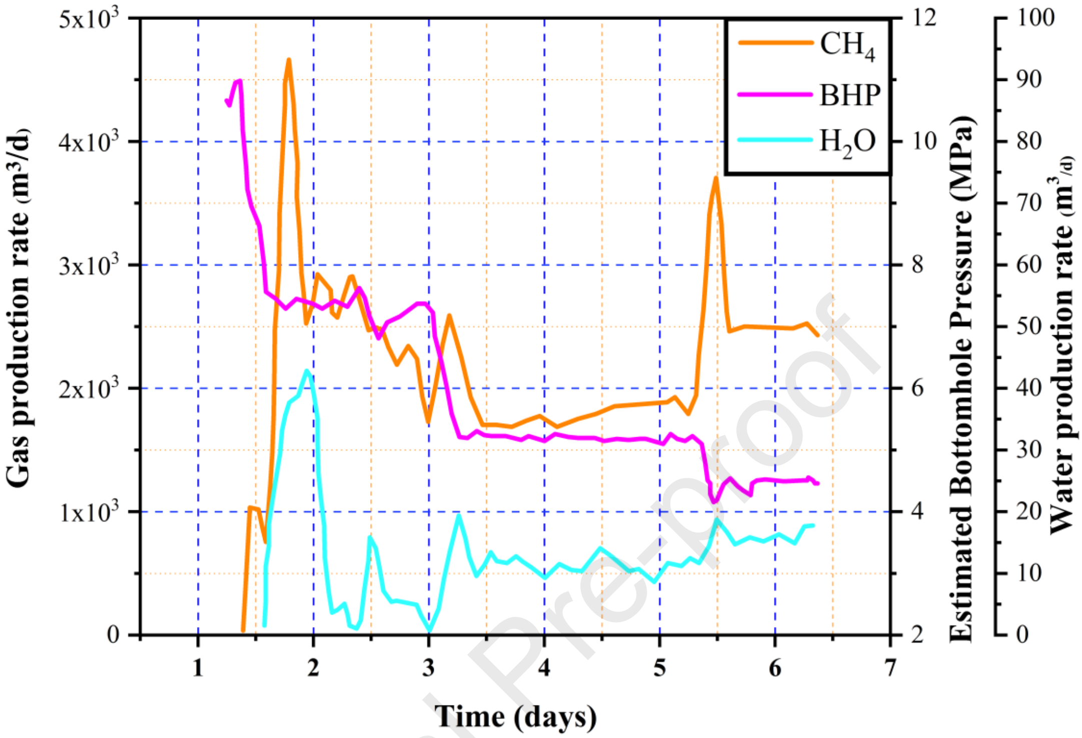

Figure 15. Gas production rate by depressurization at Mallik modified from (Kurihara, Sato, 2010) bottom hole pressure.

The approach adopted in this field case study compares well with the techniques utilized in the simulation studies as reported by (Moridis and Reagan, 2007, Li, Li, 2021, Moridis, Collett, 2004, Li, Li, 2012, Moridis, Kim, 2013, Moridis, 2004b). Figure 16 shows the production of pressure and temperature at the center of the output interval for the two simulation sets. When it comes to non-decomposing methane hydrates, the temperature increases gradually at first, then rapidly and monotonically as hot H_2O from the bottom in the aquifer is pinched to the well vice versa for dissociating.

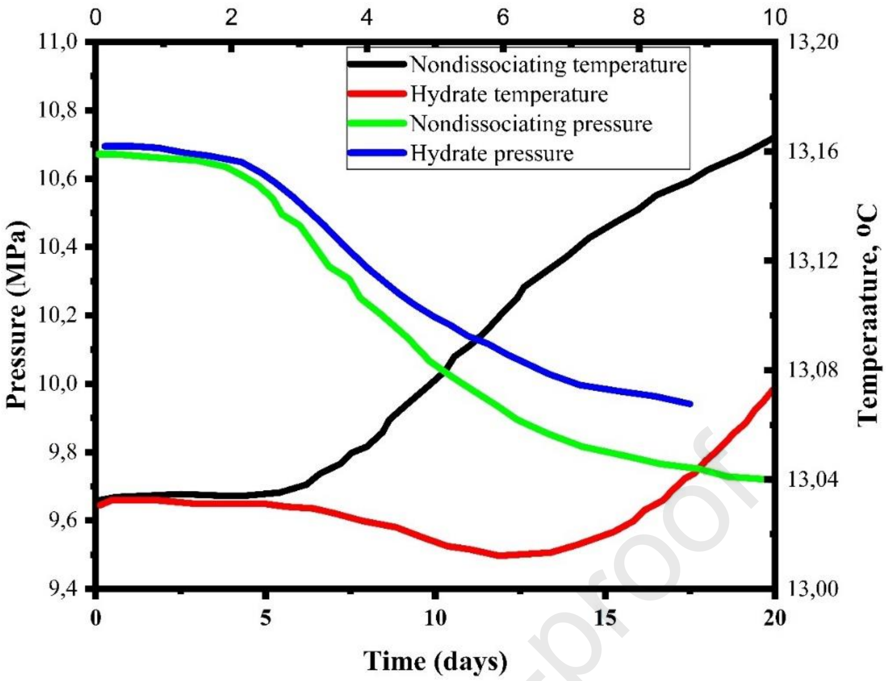

Figure 16. Pressure and temperature development in the vertical well were changed from (Moridis, Collett, 2004)

Their results show that as reservoir pressure decreases, the methane release rate raised, with the degree of pressure reduction having a substantial effect on the CH_4 release rate. Furthermore, as the temperature of the reservoir rises, so does the rate of gas release. Permeability, on the other hand, influences gas flow, so a high absolute permeability indicates a high gas flow.

4.3 Ignik Sikumi

Depressurization and CO_2 swapping procedures were applied in the current field trial production at Ignik Sikumi. A mixture of CO_2 and N_2 (a mixture ratio of 77% CO_2:23% N_2), 5946.54 m^3 was injected in a single vertical well of the reservoir (Chong, Yang, 2016, Boswell, Schoderbek, 2017a, Boswell, 2012). The injectivity pressure was 9800 kPa, with an average reservoir temperature of 5 °C that decreased as you went further into the reservoir before stabilizing at (1 to 1.5 °C). The injectivity pattern depends on the permeability from 5.5 mD to 0.6 mD and gas hydrate saturation of 0.72. Then followed by decreasing of pressure from 9800 kPa to 8270 kPa of the bottom hole. During 6 weeks 24210.9 m^3 of methane, water produced 180.7 m^3, and sand 10.65 m^3 were produced as shown in Figure 17. The use of CO_2/N_2 mixture resolved the destabilization of gas hydrate that may affect gas production. During the process, 60% of the injected CO_2 and 30% of the injected N_2 were replaced CH_4 and stored in the reservoir which is an added advantage of this technique (Boswell, Schoderbek, 2017b).

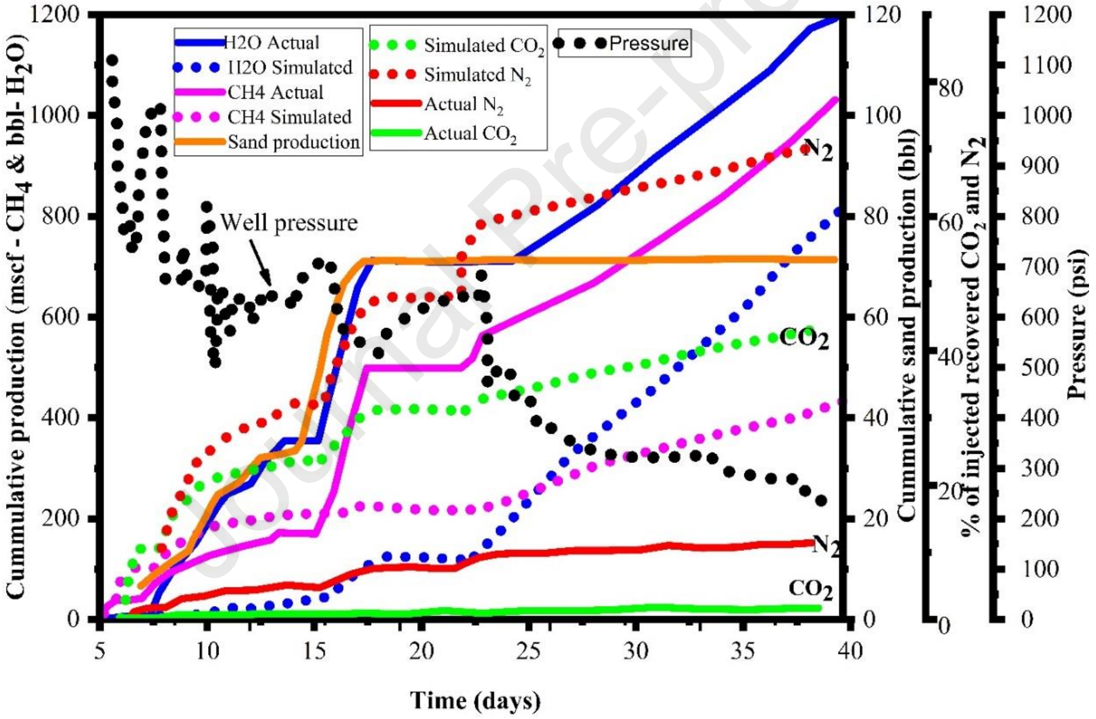

Figure 17. Development of produced H_2O: CH_4 during the Iġnik Sikumi test modified from (Boswell, Schoderbek, 2017b).

Contrary, from TOUGH-Fx/ Hydrate' (Boswell, Schoderbek, 2017b) and HydrateResSim (Garapati, McGuire, 2013) were 77% for N_2 and 23% for CO_2 that dissolved in methane hydrate reservoir, and 70% of the injected N_2 gas and 40% of the injected CO_2 were recovered, showing that CO_2 retention is preferred over CH_4 recovery in the reservoir. The model, on the other hand, predicts 39% of N_2 and 36% of CO_2 recovered (Schoderbek, Martin, 2012). The simulation's estimate of lower concentrations of N_2 and CO_2 maybe because some have been dissolved in hydrate in the reservoir. Large cages of sI hydrate are filled with primarily CO_2 during replacement processes in experimental experiments, while tiny cages are filled with N_2 (Merey, Al-Raoush, 2018, Xu, Cai, 2018). Also, the heat emitted during the production of CO_2 hydrate is 20% higher than the heat required to dissociate CH_4 hydrate (Phale, Zhu, 2006). Pressure reduced from 9800 kPa to 8300 kPa, which affects the total product of actual and model for CH_4, CO_2, and N_2 as indicated in Figure 18. The product was 13875.25 m^3 of methane, water produced 509.7 m^3 of CO_2, and sand 1812.3 m^3 of N_2 were lower produced. The results of field tests revealed that CH_4 - CO_2 exchange did occur in the solid process. Strong hydrate grains were possibly among the reservoir solids observed in the wellbore, in addition to sands and fines.

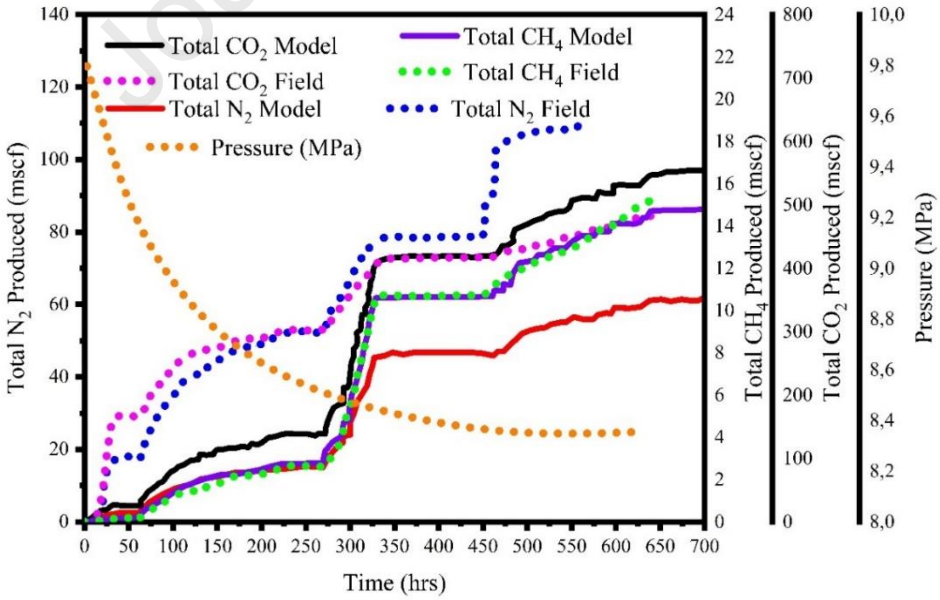

Figure 18. Effect of depressurization in production of field and model for CH_4, CO_2, and N_2

The production of CH_4 can be maximized when using fracturing that will increase the flow of methane hydrate in the reservoir. Also, the use of dual-well arrangements, like different horizontal wells joining to one vertical well that a producer together with rapidly reducing pressure also, many horizontal wells join to make one with reducing pressure or combined CO_2 swamping will improve production.

4.4 Nankai Trough

One of the case studies on the field of methane production is reported by (Konno, Fujii, 2017, Yamamoto, Terao, 2014) from the 2013 Nankai Trough test that was the 1st world's offshore CH_4 - hydrate production test. Production is done through the depressurization process in a single vertical well. The factor considered were porosity, permeability, pressure, saturation, and sand/silt of the reservoir. During the first day, the wellbore pressure was reduced from 13400 kPa to about 5000 kPa and remained steady for the next four days. During the last two days, it was further reduced to 4300 kPa as shown in Figure 19. The total production volume of 1,250 m^3 of water, 119,500 m^3 of methane gas, and 30 m^3 of sands were produced. The methane recovery was $2.0 \, x \, 10^4$ STm^3/day in 6 days, then the process stopped due to the high production of sand. Simulation is done by MH21-HYDRES by considering the following parameters porosity 0.2 – 0.6, effective permeability 0.01 to 10 mD, absolute permeability more than 1000 mD, hydrate saturation 0.7. The rate of methane output was higher than expected based on numerical simulation results. The results indicate that lithofacies and petrophysical constraints such as hydrate saturation and effective permeability have a significant impact on the dissociation and flow of methane hydrate in the reservoirs.

In May 2017, the test resumed by warming-up and depressurization method using two separated single vertical wells and two types of sand-proof designs (Chen, Feng, 2018b, Yu, Guan, 2019a, Yu, Guan, 2019c, Yu, Guan, 2019d). The 1st well was produced for 12 days before being blocked due to sand production and the possibility of increased bottom well pressure and methane hydrate regeneration. From top to bottom, there are three subzones: The upper sand/silt alternate layer has a hydrate saturation of 0.60 with intrinsic permeabilities ranging from 500 to 1100 mD, the middle silt layer has a hydrate saturation of 0.35 with intrinsic permeabilities ranging from 20 to 40 mD, and the sand-dominated layer has a hydrate saturation of 0.7. The water-bearing layer was composed of fine and very fine sand/sandy silt with intrinsic permeabilities ranging from 800 to 1000 mD, which corresponded to the lower sand-dominated layers of the Methane hydrate reservoir. The total gas output is estimated to be around 3.5 x 10^4 ST m^3, while the total water output is around 923 m^3. The second well was drilled, and flow tests were conducted for 24 days in the absence of sand output problems, with total CH_4 production estimated at 2.0 x 10^5 ST m^3 and total H_2O production estimated at 8247 m^3. On the other hand, TOUGH + HYDRATE was used to compare the result with field case production. The wellbore pressures used in the simulator were reduced from 8000 kPa to 4500 kPa, Porosity 0.4 - 0.43, saturation 0.6 - 0.70, permeability 10 – 1100 mD, and water salinity 0.035.

On the other hand, Figure 19 shows the cumulative gas production simulation result, for the P2 well was 2.17 x 10^5 ST m^3, which was 8.5 percent higher than the actual field test results of 2.0 x 10^5 ST m^3 in 2017. In addition, since the simulated H_2O output volume after modification (V_W) coincides with the actual field test results of wells, a correction factor of W = 0.3 was used in simulation outcomes correlated with the H_2O production rate (Q_W). The cumulative CH_4 performance calculated by the model for well P3 was 3.74 x 10^4 ST m^3, which matched the real field test results of 3.5 x 10^4 ST m^3. Finally, there was a substantial difference between the simulated H_2O production potential and the actual field test performance, even after correcting for the correction factor W = 0.3. The two stages of sand processing during the production test most likely contributed to this.

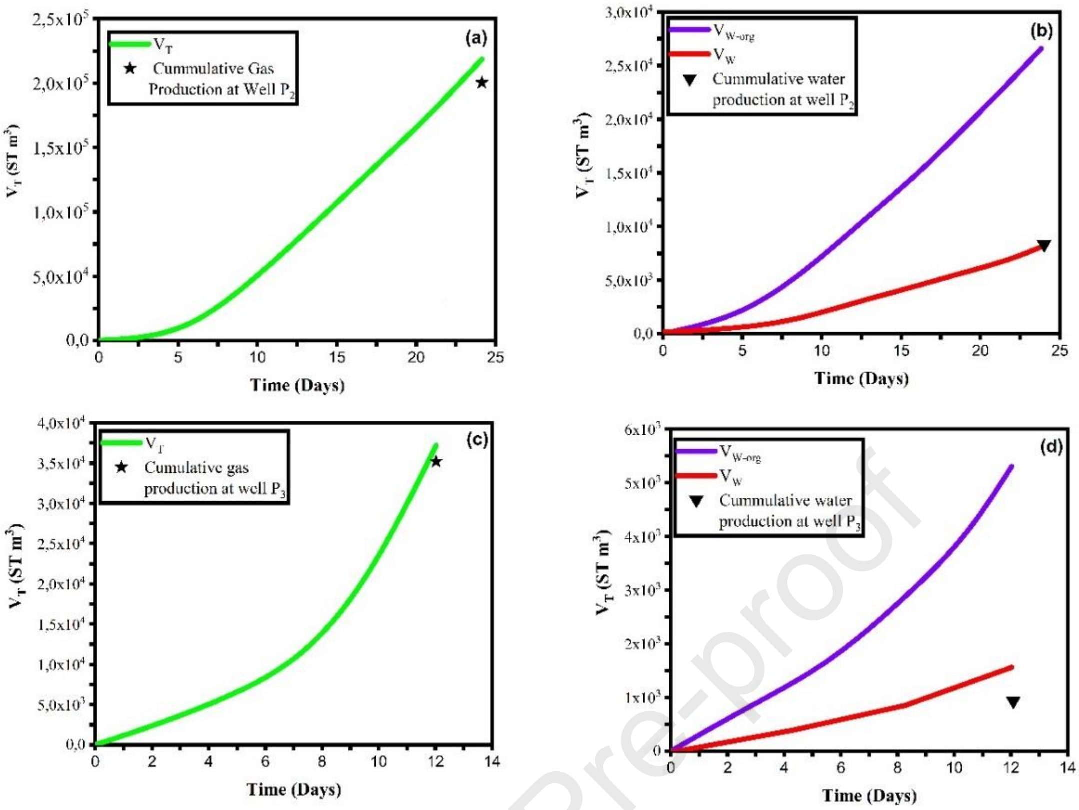

Figure 19. Simulation outcomes of cumulative CH_4 and H_2O output at two wells P2 with P3 were related to real field test data from the Nankai Trough production test 2017 modified from (Yu, Guan, 2019a).

Figure 20 indicates the approximate maximum rate of CH_4 production from methane hydrate Q_R to be 1.36 x 10^4 ST m^3/day start decreasing, whereby the rate of CH_4 from the reservoir Q_T was increased up to 1.25 x 10^4 ST m^3/day then start to decrease. Also, the rate of production of CH_4 in the gas Q_G process was raised to 8.32 x 10^3 ST m^3/day then drop down but the rate of water production from the reservoir (Q_W) was increasing from 0 to 1.35 x 10^3 ST m^3/day continuously. This is due to the dissociation of methane hydrate-release water in the reservoir. Q_R and Q_T are likely equivalents, this shows that CH_4 production initiated from hydrate dissociation. The endothermic behavior of methane hydrate dissociation creates the gap between Q_T and Q_G because of the decrease in temperature in the reservoir. This may be due to formation lithology that contains three-layer which can contribute sand and clay from each layer hance affect permeability and saturation of methane hydrate. In addition, production interval was not considered in simulation because some wellbore will be protected with packers to stop H_2O production (Yu, Guan, 2019a).

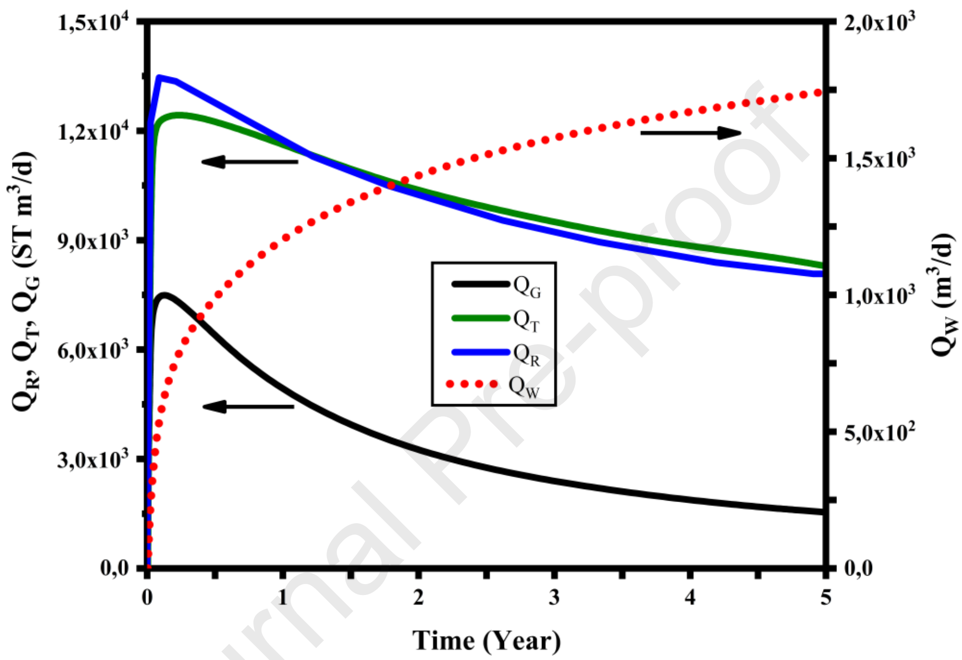

Figure 20. Production of Q_R, Q_T, Q_G, and Q_W in CH_4 - hydrate for well P_2 by depressurization modified from (Yu, Guan, 2019a).

On other hand, the pressure was not applied on time in real production like in simulation where wellbore pressure was applied immediately and cause more production of methane at an early stage. Nankai output was projected to be 10100 – 12100 ST m^3/day in five years, that was on the equivalent level of magnitude like the 2000 ST m^3/day recorded in the 2013 production test and far higher than the 2920 – 8330 ST m^3/day verified in the 2017 production test, but lower than commercial production stage 300000 ST m^3/day (Yu, Guan, 2019a). (Feng, Chen, 2019) deal with CH_4 production activities using multilayered methane hydrate deposit for vertical and horizontal wells, the horizontal well came out on top, with a significantly higher average gas output rate. Also, (Yu, Guan, 2019b) dual-well systems were used, such as dual vertical wells with rapidly reducing pressure and dual horizontal wells with reducing pressure or hot water injection. Generally, depressurization when combining with other techniques like thermal, or CO_2 injection maximizes the production rate in class 2 methane hydrate reservoirs. Dual vertical wells, horizontal wells, and a combination of depressurization and hot water injection or a combination of depressurization and CO_2 injection can all help to increase methane output. Although the combination of CO_2 and thermal methods is not effective in all classes due to the change of state of CO_2 when temperature change.

4.5 Shenhu

From May 10 to July 9, 2017, another field test was conducted in the Shenhu region of the South China Sea, which is a class 3 methane hydrate reservoir. The depressurization and thermal techniques were used. A few parameters that are considered in this reservoir were fine-grain/silty, porosity 0.4, hydrate saturation 0.3 – 0.5, lower permeability 10 – 200 mD, pressure reduced from reservoir 15000 to production pressure 4500, and temperature 12.76 °C. China was the first country to produce $3.0 \, x \, 10^5$ m^3 of methane gas for 60 days (at a rate of about $5 \, x \, 10^3$ m^3/day) Figure 21 (Chen, Feng, 2018b). However, the production stopped again due to the re-formation effects of methane hydrate (Chen, Feng, 2018a). An overall methane production rate level from methane hydrates is estimated at 3000 - 8000 m^3/day reported that was lower from the projected result for economic profit in methane hydrate which is $5.0 \, x \, 10^6$ m^3/day (Sloan, 2003). To maximize the production of methane in this field case use of combination methods like depressurization, thermal and fracturing can increase flowability. Also, a combination of CO_2 injection and depressurization will maximize the production and help to store a huge amount of CO_2 by forming $CO_2 – H_2O$ with the release of CH_4.

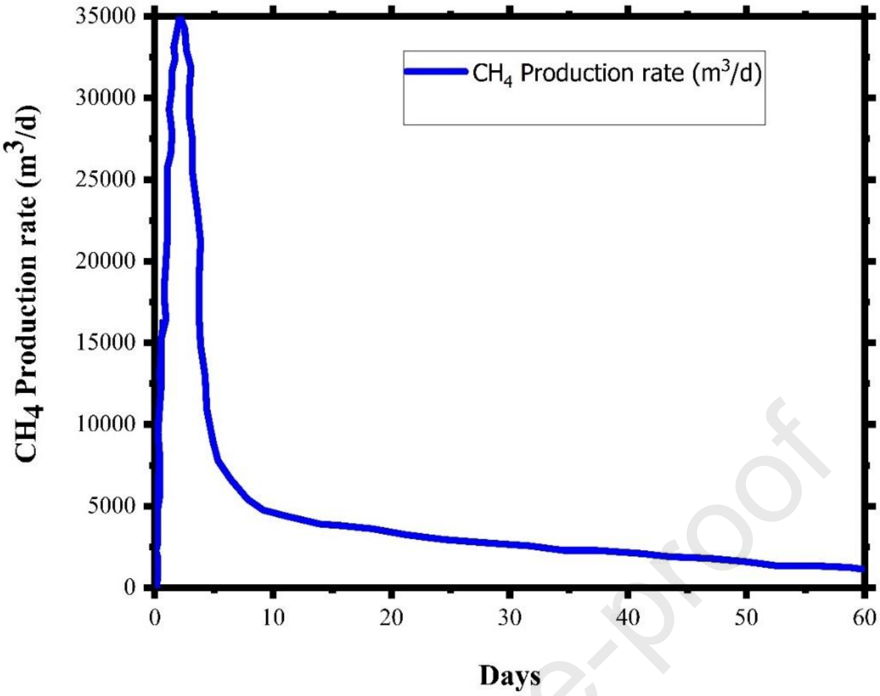

Figure 21. Shenhu test (Chen, Feng, 2018a).

On the other hand, (Yu, Guan, 2021) used TOUGH + HYDRATE to study numerical analysis based on the real methane hydrate reservoir found in Shenhu's well SHSC-4. The hydrate-bearing zone, 3 phase deposit, and free gas zone that make sublayers in a multi-layered methane hydrate reservoir model were considered. Also, changing the intrinsic permeability in different multi-layer. Their average CH_4 production rate (1.83 x 10^3 ST m^3 /day) in 2000 days as shown in Figure 22 was a lesser amount than what was reported during the 2017 Shenhu production test (5.15 x 10^3 ST m^3 /day) for long-term simulation. The majority of the overall gas output was found to come from free gas (56.5%), accompanied by CH_4 emitted from hydrate breakdown (24.1%), and the three-phase layer donated the minimum to CH_4 recovery (19.4%). In addition, the production rate of CH_4 from methane hydrate depends on intrinsic permeability. Increase intrinsic permeability promote the dissociation and flow of methane in different mechanism in a different layer.

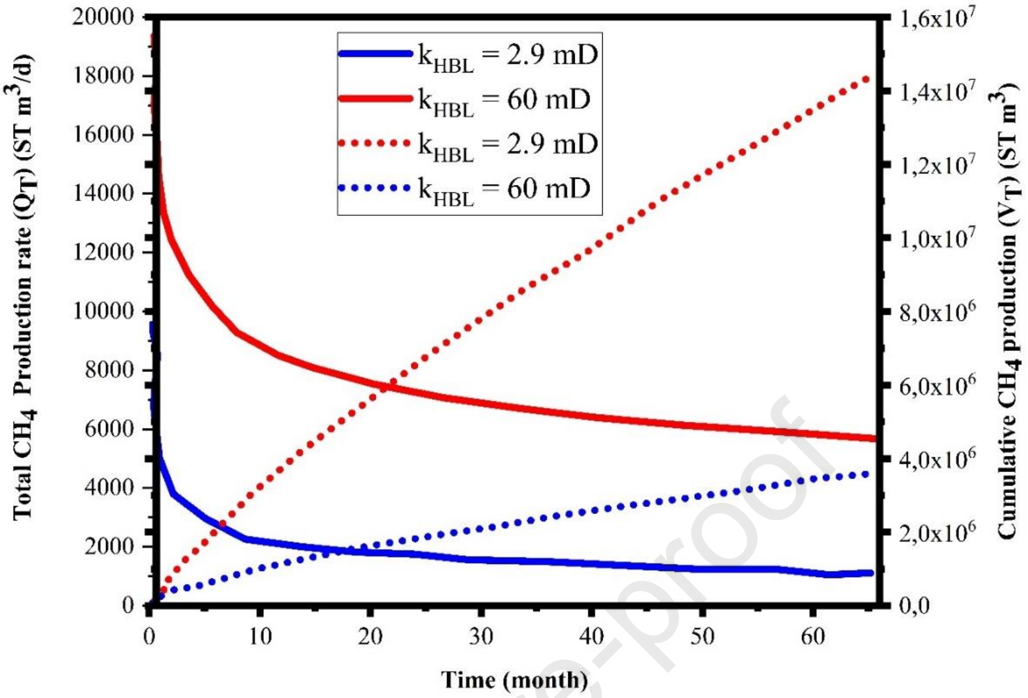

Figure 22. The production rate in TOUGH + Hydrate simulator, modified from (Chen, Feng, 2018a).

For field case production, methane production is still at a low efficiency with most challenges associated with sand production during production time, the rise of bottom-well pressure due to sand, and re-formation of the hydrate. Also, the use of horizontal wells, dual vertical wells together with rapid reduction of pressure, in addition, dual horizontal wells will maximize production in all field cases. Generally, each field case has its features or reservoir conditions, therefore the methods of recovery methane will differ, but depressurization and combination methods seem to operate in all classes. However, a combination of thermal and CO_2 injection in the class 3 methane reservoir is not efficient due to the change of state of CO_2 when temperature change. Collectively, these are some of the challenges that still limit field production of methane from methane hydrate reservoirs.

Table 10

977 Summary of field case methane production

Field case	Methods	CH_4 Produced	Challenges	References
Messoyakha	Depressurization, Thermal, and Chemical injection	Average production rate ranged 18,000 to 98,000 m^3 /day	-Increase reservoir pressure	(Makogon and Omelchenko, 2013)
Mallik	Combination of depressurization and thermal with	methane production ranged from 2000-3000 m^3 /day in 6 days	-Sand production -methane hydrate re-formation	(Kurihara, Sato, 2010)
Ignik Sikumi	Combination of depressurization with CO_2 and N_2 Injection	methane rates improved from 566.41 m^3/day to 1274.43 m^3/day in 30 days	Fine sand and water production	(Chong, Yang, 2016, Boswell, Schoderbek, 2017a, Boswell, 2012)
Nankai Trough	Depressurization with sand-proof designs	2.0×10^4 m^3/day in 6 days	-Sand formation -potential increase in bottom well pressure - CH_4 - hydrate re-formation	(Konno, Fujii, 2017, Yamamoto, Terao, 2014)

Shenhu	Combination of depressurization and thermal	maximum 3.5 × 10^4 m^3/day declines below to 2.2 *x* 10^3 m^3/day in 60 days	re-formation effects of methane hydrate inflow hot water changed the temperature of reservoirs	(Chen, Feng, 2018a).

Conclusions

This study reviewed different numerical reservoir simulators, and field trial tests to investigate the potential of methane production from various classes of methane hydrate reservoirs. Among many simulators evaluated such as MH-21, HydrateResSim, STOMP, and so on, CMG STARS and TOUGH+HYDRATE are commonly used simulators for the prediction of methane production from methane hydrates. Due to the ability to measure mass and energy balance, mass accumulation, heat accumulation, the flow of multiphase fluids, thermal, steam additives, and geomechanical fluids, source and sink, and inhibitor.

1. The methane hydrate classes discussed show that recovering methane through the use of tested methods like depressurization, thermal, CO_2 injection, chemical inhibitor, class 1 produces a significant amount in comparison to class 2 and class 3 hydrate reservoirs.

2. The suitable technique for the exploitation of methane gas in class 1 is depressurization, Class 2 is a combination of depressurization with thermal or depressurization with CO_2 injection, and Class 3 is a combination of fracking, depressurization, and CO_2 injection. But the combination of CO_2 and thermal methods are not effective in all class due to change of state of CO_2 when temperature change.

3. The maximum cumulative of methane by depressurization is 75%, thermal 49.06%, and CO_2 injection 64% combination method 87.5%.

4. The simulation analysis considered various factors like porosity, permeability, gas saturation, pressure, temperature, and so on. The pressure drops, temperature, and permeability significantly affects gas production from all methane hydrate classes. As reservoir pressure increases, the gas release rate decreases, while as the temperature of the reservoir rises methane hydrate dissociation increases hance the rate of the methane gas release increases. Permeability, on the other hand, influences gas flow, so a high absolute permeability indicates a high gas flow. The most significant impacts on the recovery of methane from methane hydrates were absolute permeability, bottom-hole pressure, and the thermal conductivity of the rock.

5. The challenges such as sand production, reformation of hydrate near the wellbore, the rise of bottom well pressure, geomechanical effects, are found to limit the maximum production of methane from methane hydrate deposit in all simulation and field trials tests. Other challenges like the effect of changes of salinity during methane production in the reservoir are not considered though several reports suggest that due to its nature it can potentially affect gas production. These observations suggest further researches need to be done to realize the maximum exploration of methane gas hydrate. We also recommend future simulation studies to consider the identifies limitations to enhance gas production from methane hydrate reservoirs.

NOMENCLATURES

Abbreviation	Meaning
CMG	Computer modeling group limited
HBL	hydrate-bearing layer
HRS	HydrateResSim

HYD	Hydrate
NGH	Natural gas hydrate
MH	methane hydrate
SH0	hydrate saturation
STOMP	Subsurface transport over multiple phases simulator
STP	Standard temperature pressure
USGS	United states geological survey
T+H	TOUGH+HYDRATE

References

[1] Davy, H., *I. The Bakerian Lecture. On some of the combinations of oxymuriatic gas and oxygene, and on the chemical relations of these principles, to inflammable bodies.* Philosophical Transactions of the Royal Society of London, 1811(101): p. 1-35.

[2] Hammerschmidt, E., *Formation of gas hydrates in natural gas transmission lines.* Industrial & Engineering Chemistry, 1934. **26**(8): p. 851-855.

[3] Makogon, Y.F., *Hydrate formation in the gas-bearing beds under permafrost conditions.* Gazovaia Promyshlennost, 1965. **5**: p. 14-15.

[4] Bily, C. and J. Dick, *Naturally occurring gas hydrates in the Mackenzie Delta, NWT.* Bulletin of Canadian Petroleum Geology, 1974. **22**(3): p. 340-352.

[5] Sloan, E.D. and C. Koh, *Hydrates of natural gases*. 1998, Marcel Dekker Inc, New York, USA.

[6] Collett, T., *Natural Gas Hydrates: Vast Resources, Uncertain Future*. 2001: US Geological Survey.

[7] Walsh, M.R., et al., *Preliminary report on the commercial viability of gas production from natural gas hydrates.* Energy Economics, 2009. **31**(5): p. 815-823.

[8] Vysniauskas, A. and P. Bishnoi, *A kinetic study of methane hydrate formation.* Chemical Engineering Science, 1983. **38**(7): p. 1061-1072.

[9] Kim, H., et al., *Kinetics of methane hydrate decomposition.* Chemical engineering science, 1987. **42**(7): p. 1645-1653.

[10] Zhao, J., et al., *Heat Transfer Analysis of Methane Hydrate Sediment Dissociation in a Closed Reactor by a Thermal Method.* Energies, 2012. **5**(5): p. 1292-1308.

[11] Makogon, Y.F., *Natural gas hydrates–A promising source of energy.* Journal of Natural Gas Science and Engineering, 2010. **2**(1): p. 49-59.

[12] Makogon, Y.F. and R.Y. Omelchenko, *Commercial gas production from Messoyakha deposit in hydrate conditions.* Journal of Natural Gas Science and Engineering, 2013. **11**: p. 1-6.

[13] Moridis, G., et al., *Gas production from a cold, stratigraphically-bounded gas hydrate deposit at the Mount Elbert Gas Hydrate Stratigraphic Test Well, Alaska North Slope: Implications of uncertainties.* Marine and petroleum geology, 2011. **28**(2): p. 517-534.

[14] Ruppel, C.D., *Methane hydrates and contemporary climate change.* Nature Eduction Knowledge, 2011. **2**(12): p. 12.

[15] Kurihara, M., et al., *Analysis of Production Data for 2007/2008 Mallik Gas Hydrate Production Tests in Canada*, in *International Oil and Gas Conference and Exhibition in China*. 2010, Society of Petroleum Engineers: Beijing, China. p. 24.

[16] Garapati, N., P. McGuire, and B.J. Anderson, *Modeling the Injection of Carbon Dioxide and Nitrogen into a Methane Hydrate Reservoir and the Subsequent Production of Methane Gas on the North Slope of Alaska*, in *Unconventional Resources Technology Conference, Denver, Colorado, 12-14 August 2013*. 2013, Society of Exploration Geophysicists, American Association of Petroleum Geologists, Society of Petroleum Engineers. p. 1942-1951.

[17] Konno, Y., et al., *Key Findings of the World's First Offshore Methane Hydrate Production Test off the Coast of Japan: Toward Future Commercial Production.* Energy & Fuels, 2017. **31**(3): p. 2607-2616.

[18] Yamamoto, K., et al., *Operational overview of the first offshore production test of methane hydrates in the Eastern Nankai Trough*, in *Offshore Technology Conference*. 2014, Offshore Technology Conference: Houston, Texas. p. 11.

[19] Chen, L., et al., *Production behavior and numerical analysis for 2017 methane hydrate extraction test of Shenhu, South China Sea.* Journal of Natural Gas Science and Engineering, 2018a. **53**: p. 55-66.

[20] Chen, L., et al., *Construction and simulation of reservoir scale layered model for production and utilization of methane hydrate: The case of Nankai Trough Japan.* Energy, 2018b. **143**: p. 128-140.

[21] Moridis, G.J., M. Kowalsky, and S. Finsterle, *TOUGH-Fx*. 2005a, Lawrence Berkeley National Laboratory.

[22] Oyama, A. and S. Masutani, *A review of the methane hydrate program in Japan.* Energies, 2017. **10**(10): p. 1447.

[23] Moridis, G., M. Kowalsky, and K. Pruess, *HydrateResSim Users Manual: A Numerical Simulator for Modeling the Behavior of Hydrates in Geologic Media.* Earth Sciences Division, Lawrence Berkeley National Laboratory, Berkeley, CA, 2005b. **94720**.

[24] Moridis, G., M. Kowalsky, and K. Pruess, *Users Manual: a Numerical Simulator for Modeling the Behavior of Hydrates in Geologic media/HydrateResSim. Department of Energy.* Contract No. DE-AC03-76SF00098.—Lawrence Berkeley National Laboratory, Berkeley, CA, 2005c.

[25] Stars, C., *Computer Modeling Group Ltd.* Calgary, Alberta, Canada, 2007.

[26] White, M. and M. Oostrom, *STOMP subsurface transport over multiple phases, version 4.0, user's guide. PNNL-15782. Pacific Northwest National Laboratory, Richland, WA.* STOMP subsurface transport over multiple phases, version 4.0, user's guide. PNNL-15782. Pacific Northwest National Laboratory, Richland, WA., 2006: p. -.

[27] Kvenvolden, K.A., *Methane hydrates and global climate.* Global biogeochemical cycles, 1988. **2**(3): p. 221-229.

[28] Makogon, Y.F., S. Holditch, and T.Y. Makogon, *Natural gas-hydrates—A potential energy source for the 21st Century*. Journal of petroleum science and engineering, 2007. **56**(1-3): p. 14-31.

[29] Kumar, R. and P. Linga, *Gas Hydrates*, in *Encyclopedia of Geochemistry: A Comprehensive Reference Source on the Chemistry of the Earth*, W.M. White, Editor. 2017, Springer International Publishing: Cham. p. 1-7.

[30] Majorowicz, J. and K. Osadetz, *Gas hydrate distribution and volume in Canada.* AAPG bulletin, 2001. **85**(7): p. 1211-1230.

[31] Osadetz, K. and Z. Chen. *A re-examination of Beaufort Sea-Mackenzie delta basin gas hydrate resource potential using a petroleum play approach*. in *Proceedings of the 5th International Conference on Gas Hydrate*. 2005.

[32] Bird, K.J. and L.B. Magoon, *Petroleum geology of the northern part of the Arctic National Wildlife Refuge, northeastern Alaska*. 1987: US Government Printing Office.

[33] Collett, T.S., *Natural gas hydrates of the Prudhoe Bay and Kuparuk River area, north slope, Alaska.* AAPG bulletin, 1993. **77**(5): p. 793-812.

[34] Collett, T.S., *Arctic gas hydrate energy assessment studies.* The Arctic Energy Summit, Anchorage, Alaska, 2007: p. 15-18.

[35] Makogon, I.U.r.F., *Hydrates of natural gas*. 1981: PennWell Books Tulsa, Oklahoma.

[36] ZHU, Y., et al., *Gas Hydrates in the Qilian Mountain Permafrost, Qinghai, Northwest China.* Acta Geologica Sinica - English Edition, 2010. **84**(1): p. 1-10.

[37] Takahashi, H., T. Yonezawa, and Y. Takedomi. *Exploration for natural hydrate in Nankai-Trough wells offshore Japan*. in *Offshore Technology Conference*. 2001. Offshore Technology Conference.

[38] Takahashi, H. and Y. Tsuji. *Multi-well exploration program in 2004 for natural hydrate in the Nankai-Trough offshore Japan*. in *Offshore Technology Conference*. 2005. Offshore Technology Conference.

[39] Fujii, T., et al. *Resource assessment of methane hydrate in the eastern Nankai Trough, Japan*. in *Offshore technology conference*. 2008. Offshore Technology Conference.

[40] Kurihara, M., et al. *Prediction of gas productivity from eastern Nankai Trough methane hydrate reservoirs*. in *Offshore technology conference*. 2008. Offshore Technology Conference.

[41] Saeki, T., et al. *Extraction of methane hydrate concentrated zone for resource assessment in the eastern Nankai Trough, Japan*. in *Offshore Technology Conference*. 2008. Offshore Technology Conference.

[42] Moridis, G.J. and M.T. Reagan, *Strategies for gas production from oceanic class 3 hydrate accumulations.* 2007.

[43] Ye, J.-l., et al., *The second natural gas hydrate production test in the South China Sea.* China Geology, 2020. **3**(2): p. 197-209.

[44] Sloan, E.D. and C. Koh, *Clathrate hydrates of natural gases*. 2007.

[45] McMullan, R.K. and G. Jeffrey, *Polyhedral clathrate hydrates. IX. Structure of ethylene oxide hydrate.* The Journal of Chemical Physics, 1965. **42**(8): p. 2725-2732.

[46] Ripmeester, J.A., et al., *A new clathrate hydrate structure.* Nature, 1987. **325**(6100): p. 135-136.

[47] Moridis, G. and T. Collett, *Strategies for gas production from hydrate accumulations under various geologic conditions.* 2003.

[48] Moridis, G.J., *Toward production from gas hydrates: current status, assessment of resources, and simulation-based evaluation of technology and potential.* 2008.

[49] Moridis, G.J. and E.D. Sloan, *Gas production potential of disperse low-saturation hydrate accumulations in oceanic sediments.* Energy conversion and management, 2007. **48**(6): p. 1834-1849.

[50] Moridis, G.J., M.B. Kowalsky, and K. Pruess, *Depressurization-induced gas production from class-1 hydrate deposits.* SPE Reservoir Evaluation & Engineering, 2007. **10**(05): p. 458-481.

[51] Bhade, P. and J. Phirani, *Gas production from layered methane hydrate reservoirs.* Energy, 2015. **82**: p. 686-696.

[52] Kurihara, M., et al. *Gas production from methane hydrate reservoirs*. in *Proceedings of the 7th International Conference on Gas Hydrates (ICGH 2011), Edinburgh, Scotland, United Kingdom*. 2011.

[53] Lin, C., et al., *A review analysis of gas hydrate tests: engineering progress and policy trend.* Environmental Geotechnics. **0**(0): p. 1-17.

[54] Xu, C.-G. and X.-S. Li, *Research progress on methane production from natural gas hydrates.* RSC advances, 2015. **5**(67): p. 54672-54699.

[55] Su, Z., et al., *Evaluation on gas production potential from laminar hydrate deposits in Shenhu Area of South China Sea through depressurization using vertical wells.* Journal of Petroleum Science and Engineering, 2012. **86-87**: p. 87-98.

[56] Konno, Y., et al., *Key Factors for Depressurization-Induced Gas Production from Oceanic Methane Hydrates.* Energy & Fuels, 2010. **24**(3): p. 1736-1744.

[57] Holder, G., et al., *A thermodynamic evaluation of thermal recovery of gas from hydrates in the earth (includes associated papers 11863 and 11924).* Journal of Petroleum Technology, 1982. **34**(05): p. 1,127-1,132.

[58] Bayles, G., et al., *A steam cycling model for gas production from a hydrate reservoir.* Chemical Engineering Communications, 1986. **47**(4-6): p. 225-245.

[59] Selim, M. and E. Sloan, *Heat and mass transfer during the dissociation of hydrates in porous media.* AIChE journal, 1989. **35**(6): p. 1049-1052.

[60] Selim, M. and E. Sloan, *Hydrate dissociation in sediment.* SPE Reservoir Engineering, 1990. **5**(02): p. 245-251.

[61] Ullerich, J., M. Selim, and E. Sloan, *Theory and measurement of hydrate dissociation.* AIChE Journal, 1987. **33**(5): p. 747-752.

[62] Tsypkin, G., *Gas hydrate dissociation regimes in highly permeable beds.* Journal of Engineering Physics and Thermophysics, 1992. **63**(6): p. 1221-1227.

[63] Tsypkin, G. *Mathematical model for dissociation of gas hydrates coexisting with gas in strata*. in *Doklady Physics*. 2001. Springer.

[64] Xu, W., *Modeling dynamic marine gas hydrate systems.* American Mineralogist, 2004. **89**(8-9): p. 1271-1279.

[65] Islam, M., *A new recovery technique for gas production from Alaskan gas hydrates.* Journal of petroleum Science and Engineering, 1994. **11**(4): p. 267-281.

[66] Jamaluddin, A., N. Kalogerakis, and P. Bishnoi, *Modelling of decomposition of a synthetic core of methane gas hydrate by coupling intrinsic kinetics with heat transfer rates.* The Canadian Journal of Chemical Engineering, 1989. **67**(6): p. 948-954.

[67] Merey, Ş. and S.N. Longinos, *Numerical simulations of gas production from Class 1 hydrate and Class 3 hydrate in the Nile Delta of the Mediterranean Sea.* Journal of Natural Gas Science and Engineering, 2018a. **52**: p. 248-266.

[68] Sung, W., et al., *Numerical study for production performances of a methane hydrate reservoir stimulated by inhibitor injection.* Energy Sources, 2002. **24**(6): p. 499-512.

[69] Kamath, V., et al., *Experimental study of brine injection depressurization of gas hydrates dissociation of gas hydrates.* SPE Formation Evaluation, 1991. **6**(04): p. 477-484.

[70] Kamath, V.A. and S.P. Godbole, *Evaluation of hot-brine stimulation technique for gas production from natural gas hydrates.* Journal of petroleum technology, 1987. **39**(11): p. 1,379-1,388.

[71] Ohgaki, K., et al., *Methane Exploitation by Carbon Dioxide from Gas Hydrates—Phase Equilibria for CO2-CH4 Mixed Hydrate System—.* Journal of chemical engineering of Japan, 1996. **29**(3): p. 478-483.

[72] Nakano, S., K. Yamamoto, and K. Ohgaki, *Natural gas exploitation by carbon dioxide from gas hydrate fields—high-pressure phase equilibrium for an ethane hydrate system.* Proceedings of the Institution of Mechanical Engineers, Part A: Journal of Power and Energy, 1998. **212**(3): p. 159-163.

[73] Smith, D.H., K. Seshadri, and J.W. Wilder, *Assessing the thermodynamic feasibility of the conversion of methane hydrate into carbon dioxide hydrate in porous media*. 2001, National Energy Technology Laboratory, Morgantown, WV (United States).

[74] McGrail, B., et al., *A new method for enhanced production of gas hydrates with CO2.* Gas hydrates: energy resource potential and associated geologic hazards, 2004. **2004**: p. 12-6.

[75] Ota, M., et al., *Replacement of CH_4 in the hydrate by use of liquid CO_2.* Energy Conversion and Management, 2005. **46**(11-12): p. 1680-1691.

[76] White, M.D. and B.P. McGrail, *Numerical Simulation of Methane Hydrate Production from Geologic Formations via Carbon Dioxide Injection*, in *Offshore Technology Conference*. 2008, Offshore Technology Conference: Houston, Texas, USA. p. 12.

[77] Deusner, C., et al., *Methane production from gas hydrate deposits through injection of supercritical CO_2.* Energies, 2012. **5**(7): p. 2112-2140.

[78] Handa, Y., *Compositions, enthalpies of dissociation, and heat capacities in the range 85 to 270 K for clathrate hydrates of methane, ethane, and propane, and enthalpy of dissociation of isobutane hydrate, as determined by a heat-flow calorimeter.* The Journal of chemical thermodynamics, 1986. **18**(10): p. 915-921.

[79] Kang, S.-P., H. Lee, and B.-J. Ryu, *Enthalpies of dissociation of clathrate hydrates of carbon dioxide, nitrogen,(carbon dioxide+ nitrogen), and (carbon dioxide+ nitrogen+ tetrahydrofuran).* The Journal of Chemical Thermodynamics, 2001. **33**(5): p. 513-521.

[80] Janicki, G., et al., *Simulation of subsea gas hydrate exploitation.* Energy Procedia, 2014. **59**(2014): p. 82-89.

[81] Duan, S., et al., *Adsorption equilibrium of CO_2 and CH_4 and their mixture on Sichuan Basin shale.* Energy & Fuels, 2016. **30**(3): p. 2248-2256.

[82] Merey, S., et al., *Comprehensive literature review on CH_4-CO_2 replacement in microscale porous media.* Journal of Petroleum Science and Engineering, 2018. **171**: p. 48-62.

[83] Yousif, M., et al., *Experimental and theoretical investigation of methane-gas-hydrate dissociation in porous media.* SPE reservoir Engineering, 1991. **6**(01): p. 69-76.

[84] Yousif, M. and E. Sloan, *Experimental investigation of hydrate formation and dissociation in consolidated porous media.* SPE Reservoir Engineering, 1991. **6**(04): p. 452-458.

[85] Sung, W.-M., et al., *Development and application of gas hydrate reservoir simulator based on depressurizing mechanism.* Korean Journal of Chemical Engineering, 2000. **17**(3): p. 344-350.

[86] Goel, N., M. Wiggins, and S. Shah, *Analytical modeling of gas recovery from in situ hydrates dissociation.* Journal of Petroleum Science and Engineering, 2001. **29**(2): p. 115-127.

[87] Khataniar, S., et al., *Modelling and economic analysis of gas production from hydrates by depressurization method.* The Canadian Journal of Chemical Engineering, 2002. **80**(1): p. 135-143.

[88] Ahmadi, G., C. Ji, and D.H. Smith, *Numerical solution for natural gas production from methane hydrate dissociation.* Journal of petroleum science and engineering, 2004. **41**(4): p. 269-285.

[89] Hong, H. and M. Pooladi-Darvish. *A numerical study on gas production from formations containing gas hydrates*. in *Canadian International Petroleum Conference*. 2003. Petroleum Society of Canada.

[90] Hong, H. and M. Pooladi-Darvish, *Simulation of Depressurization for Gas Production From Gas Hydrate Reservoirs.* Journal of Canadian Petroleum Technology, 2005. **44**(11): p. 8.

[91] Ji, C., G. Ahmadi, and D.H. Smith, *Natural gas production from hydrate decomposition by depressurization.* Chemical Engineering Science, 2001. **56**(20): p. 5801-5814.

[92] Ji, C., G. Ahmadi, and D.H. Smith, *Constant rate natural gas production from a well in a hydrate reservoir.* Energy conversion and management, 2003. **44**(15): p. 2403-2423.

[93] Bai, D., et al., *Replacement mechanism of methane hydrate with carbon dioxide from microsecond molecular dynamics simulations.* Energy & Environmental Science, 2012. **5**(5): p. 7033-7041.

[94] Zhao, J., et al., *Analyzing the process of gas production for natural gas hydrate using depressurization.* Applied energy, 2015. **142**: p. 125-134.

[95] Moridis, G.J., *Numerical Studies of Gas Production From Methane Hydrates*, in *SPE Gas Technology Symposium*. 2002, Society of Petroleum Engineers: Calgary, Alberta, Canada. p. 14.

[96] Zhao, J., et al., *Gas production behavior from hydrate-bearing fine natural sediments through optimized step-wise depressurization.* Applied Energy, 2020. **260**: p. 114275.

[97] Liang, H., et al., *New Approach for Determining the Reaction Rate Constant of Hydrate Formation via X-ray Computed Tomography.* The Journal of Physical Chemistry C, 2021. **125**(1): p. 42-48.

[98] Ruan, X. and X.-S. Li, *Investigation of the methane hydrate surface area during depressurization-induced dissociation in hydrate-bearing porous media.* Chinese Journal of Chemical Engineering, 2021. **32**: p. 324-334.

[99] Nakayama, T., et al. *Estimation of Surface Area of Methane Hydrate In Sediments*. in *Seventh ISOPE Ocean Mining Symposium*. 2007.

[100] Lee, H., et al., *Recovering methane from solid methane hydrate with carbon dioxide.* Angewandte Chemie International Edition, 2003. **42**(41): p. 5048-5051.

[101] Zakharov, V.E., A.I. Dyachenko, and O.A. Vasilyev, *New method for numerical simulation of a nonstationary potential flow of incompressible fluid with a free surface.* European Journal of Mechanics - B/Fluids, 2002. **21**(3): p. 283-291.

[102] Swinkels, W.J. and R.J. Drenth, *Thermal reservoir simulation model of production from naturally occurring gas hydrate accumulations.* SPE Reservoir Evaluation & Engineering, 2000. **3**(06): p. 559-566.

[103] Wilder, J.W., et al. *An international effort to compare gas hydrate reservoir simulators*. in *Proceedings of 6th International Conference on Gas Hydrates (ICGH 2008), Vancouver, CANADA*. 2008.

[104] Sun, X., et al., *Numerical modeling for the mechanical behavior of marine gas hydrate-bearing sediments during hydrate production by depressurization.* Journal of Petroleum Science and Engineering, 2019. **177**: p. 971-982.

[105] Ruan, X., X.-S. Li, and C.-G. Xu, *A review of numerical research on gas production from natural gas hydrates in China.* Journal of Natural Gas Science and Engineering, 2021. **85**: p. 103713.

[106] Moridis, G.J., *Tough+Hydrate v1.5 User's Manual: A code for the simulation of system behavior in hydrate-bearing geologic media*. 2014a.

[107] CMG, E., *STARS: Users' Guide, Advanced Processes & Thermal Reservoir Simulator (Version 2015).* 2015.

[108] Kurihara, M., et al., *Assessment of gas productivity of natural methane hydrates using MH21 Reservoir Simulator*. Natural Gas Hydrates: Energy Resource Potential and Associated Geologic Hazards, 2004.

[109] Moridis, G., M. Kowalsky, and K. Pruess, *HydrateResSim Users Manual: A Numerical Simulator for Modeling the Behavior of Hydrates in Geologic Media*. 2005d.

[110] White, M.D., *STOMP subsurface transport over multiple phases, version 4.0, user's guide*. 2006.

[111] Moridis, G., M. Kowalsky, and K. Pruess, *TOUGH+ HYDRATE v1. 0 User's Manual: a code for the simulation of system behaviour in hydrate-bearing porous media.* Report LBNL-149E. Lawrence Berkeley National Laboratory, Berkeley, CA, 2008.

[112] Moridis, G.J., *User's manual for the hydrate v1. 5 option of TOUGH+ v1. 5: A code for the simulation of system behavior in hydrate-bearing geologic media*. 2014b, Lawrence Berkeley National Lab.(LBNL), Berkeley, CA (United States).

[113] Grover, T., S.A. Holditch, and G. Moridis, *Analysis of Reservoir Performance of Messoyakha Gas Hydrate Field,* in *The Eighteenth International Offshore and Polar Engineering Conference*. 2008, International Society of Offshore and Polar Engineers: Vancouver, Canada. p. 8.

[114] Clarke, M.A. and P.R. Bishnoi, *Measuring and modelling the rate of decomposition of gas hydrates formed from mixtures of methane and ethane.* Chemical Engineering Science, 2001a. **56**(16): p. 4715-4724.

[115] Clarke, M.A. and P.R. Bishnoi, *Determination of the activation energy and intrinsic rate constant of methane gas hydrate decomposition.* Can. J. Chem. Eng., 2001b. **79**: p. 143.

[116] Phale, H.A., et al. *Simulation study on injection of CO2-microemulsion for methane recovery from gas-hydrate reservoirs*. in *SPE Gas Technology Symposium*. 2006. Society of Petroleum Engineers.

[117] Sasaki, K., Y. Sugai, and T. Yamakawa. *Integrated thermal gas production from methane hydrate formation*. in *SPE/EAGE European Unconventional Resources Conference and Exhibition*. 2014. European Association of Geoscientists & Engineers.

[118] Kurihara, M. *Investigation on applicability of methane hydrate production methods to reservoirs with diverse characteristics*. in *Proc. of the Fifth International Conference on Gas Hydrates, 0000*. 2005.

[119] CMG, W., *Advanced Processes & Thermal Reservoir Simulator*. 2017, User’s Guide. CM Group. Calgary, Canada, Computer Modelling Group Ltd.

[120] Lin, T.-K. and B.-Z. Hsieh, *Prevention of Seabed Subsidence of Class-1 Gas Hydrate Deposits via CO2-EGR: A Numerical Study with Coupled Geomechanics-Hydrate Reaction-Multiphase Fluid Flow Model.* Energies, 2020. **13**(7): p. 1579.

[121] Wu, C.-Y. and B.-Z. Hsieh, *Comparisons of different simulated hydrate designs for Class-1 gas hydrate deposits.* Journal of Natural Gas Science and Engineering, 2020. **77**: p. 103225.

[122] Zhang, K., *A domain decomposition approach for large-scale simulations of flow processes in hydrate-bearing geologic media.* 2009.

[123] Moridis, G.J. and M. Kowalsky, *Depressurization-induced gas production from Class 1 and Class 2 hydrate deposits.* 2006a.

[124] Alp, D., M. Parlaktuna, and G.J. Moridis, *Gas production by depressurization from hypothetical Class 1G and Class 1W hydrate reservoirs.* Energy conversion and management, 2007. **48**(6): p. 1864-1879.

[125] Howe, S., et al., *Production modeling of a potential methane hydrate accumulation on the north slope of Alaska.* Petroleum science and technology, 2009. **27**(9): p. 923-932.

[126] Howe, S.J., *Production modeling and economic evaluation of a potential gas hydrate pilot production program on the North Slope of Alaska*. 2004.

[127] Uddin, M. and D. Coombe. *CO Hydrate Formation in Geological Reservoirs by Injection of CO Gas*. in *Canadian International Petroleum Conference*. 2007. Petroleum Society of Canada.

[128] Llamedo, M.A., et al., *Gas Production From Hydrates Dissociation in Marine Sediments,* in *SPE Latin American and Caribbean Petroleum Engineering Conference*. 2010, Society of Petroleum Engineers: Lima, Peru. p. 20.

[129] Bai, Y., et al., *Interbed patterns division and its effect on production performance for class I hydrate deposit with mudstone interbed.* Energy, 2020. **211**: p. 118666.

[130] Merey, S. and C. Sinayuc, *Investigation of gas hydrate potential of the Black Sea and modelling of gas production from a hypothetical Class 1 methane hydrate reservoir in the Black Sea conditions.* Journal of Natural Gas Science and Engineering, 2016. **29**: p. 66-79.

[131] Merey, Ş. and S.N. Longinos, *Does the Mediterranean Sea have potential for producing gas hydrates?* Journal of Natural Gas Science and Engineering, 2018b. **55**: p. 113-134.

[132] Liu, Y., et al., *Numerical simulation of simultaneous exploitation of geothermal energy and natural gas hydrates by water injection into a geothermal heat exchange well.* Renewable and Sustainable Energy Reviews, 2019. **109**: p. 467-481.

[133] Sloan Jr, E.D. and F. Fleyfel, *A molecular mechanism for gas hydrate nucleation from ice.* AIChE Journal, 1991. **37**(9): p. 1281-1292.

[134] White, M.D., S.K. Wurstner, and B.P. McGrail, *Numerical studies of methane production from Class 1 gas hydrate accumulations enhanced with carbon dioxide injection.* Marine and Petroleum Geology, 2011. **28**(2): p. 546-560.

[135] White, M. and P. McGrail, *Designing a pilot-scale experiment for the production of natural gas hydrates and sequestration of CO2 in class 1 hydrate accumulations.* Energy Procedia, 2009. **1**(1): p. 3099-3106.

[136] Sloan Jr, E.D. and C.A. Koh, *Clathrate hydrates of natural gases*. 2007: CRC press.

[137] Schoderbek, D., et al., *ConocoPhillips gas hydrate production test*. 2013, ConocoPhillips Co., Houston, TX (United States).

[138] Kvamme, B., *Feasibility of simultaneous CO2 storage and CH4 production from natural gas hydrate using mixtures of CO2 and N2.* Canadian Journal of Chemistry, 2015. **93**(8): p. 897-905.

[139] Xu, C.-G., et al., *Research on micro-mechanism and efficiency of CH4 exploitation via CH4-CO2 replacement from natural gas hydrates.* Fuel, 2018. **216**: p. 255-265.

[140] Kurihara, M., et al., *Analysis of the JAPEX/JNOC/GSC et al. Mallik 5L-38 gas hydrate thermal-production test through numerical simulation.* BULLETIN-GEOLOGICAL SURVEY OF CANADA, 2005. **585**: p. 139.

[141] Masuda, Y., et al. *Improvement of near wellbore permeability by methanol stimulation in a methane hydrate production well*. in *Offshore Technology Conference*. 2008. Offshore Technology Conference.

[142] Narita, H., *Introduction of MH21 (Research Consortium For Methane Hydrate Resources In Japan) And Current Topics In Production Method & Modeling of Methane Hydrate*, in *Fifth ISOPE Ocean Mining Symposium*. 2003, International Society of Offshore and Polar Engineers: Tsukuba, Japan. p. 5.

[143] Moridis, G.J., et al., *Gas hydrates as a potential energy source: state of knowledge and challenges*, in *Advanced Biofuels and Bioproducts*. 2013, Springer. p. 977-1033.

[144] Jenkins, J.A. and D.F. Williams, *Nile water as a cause of Eastern Mediterranean sapropel formation: Evidence for and against.* Marine Micropaleontology, 1984. **8**(6): p. 521-534.

[145] Uddin, M., D. Coombe, and F. Wright, *Modeling of CO2-hydrate formation in geological reservoirs by injection of CO2 gas.* Journal of Energy Resources Technology, 2008. **130**(3).

[146] Sun, J., et al., *Numerical simulation on gas production from hydrate reservoir at the 1st offshore test site in the eastern Nankai Trough.* Journal of Natural Gas Science and Engineering, 2016. **30**: p. 64-76.

[147] Moridis, G., *Numerical studies of gas production from Class 2 and Class 3 hydrate accumulations at the Mallik Site, Mackenzie Delta, Canada.* SPE Reservoir Evaluation & Engineering, 2004a. **7**(03): p. 175-183.

[148] Reagan, M., *Sensitivity analysis of gas production from Class 2 and Class 3 hydrate deposits.* 2009.

[149] Moridis, G.J. and M. Kowalsky, *Gas production from unconfined Class 2 oceanic hydrate accumulations*, in *Economic geology of natural gas hydrate*. 2006b, Springer. p. 249-266.

[150] Moridis, G.J. and M.T. Reagan, *Estimating the upper limit of gas production from Class 2 hydrate accumulations in the permafrost: 1. Concepts, system description, and the production base case.* Journal of Petroleum Science and Engineering, 2011. **76**(3): p. 194-204.

[151] Xia, Z., et al., *Production characteristic investigation of the Class Ⅰ, Class Ⅱ and Class Ⅲ hydrate reservoirs developed by the depressurization and thermal stimulation combined method.* Journal of Petroleum Science and Engineering, 2017. **157**: p. 56-67.

[152] Jemai, K., B. Kvamme, and M.T. Vafaei, *Theoretical studies of CO2 hydrates formation and dissociation in cold aquifers using RetrasoCodeBright simulator.* Reactive transport modelling of hydrate phase transition dynamics in porous media, 2014.

[153] Li, S., J.L. Falconer, and R.D. Noble, *SAPO-34 membranes for CO2/CH4 separation.* Journal of Membrane Science, 2004. **241**(1): p. 121-135.

[154] Cui, X., R.M. Bustin, and G. Dipple, *Selective transport of CO2, CH4, and N2 in coals: insights from modeling of experimental gas adsorption data.* Fuel, 2004. **83**(3): p. 293-303.

[155] McGrail, B.P., et al., *Using carbon dioxide to enhance recovery of methane from gas hydrate reservoirs: final summary report*. 2007, Pacific Northwest National Lab.(PNNL), Richland, WA (United States).

[156] Busch, A. and Y. Gensterblum, *CBM and CO2-ECBM related sorption processes in coal: A review.* International Journal of Coal Geology, 2011. **87**(2): p. 49-71.

[157] Ruthven, D.M., *Fundamentals of Adsorption Equilibrium and Kinetics in Microporous Solids*, in *Adsorption and Diffusion*, H.G. Karge and J. Weitkamp, Editors. 2008, Springer Berlin Heidelberg: Berlin, Heidelberg. p. 1-43.

[158] Iddphonce, R., J. Wang, and L. Zhao, *Review of CO2 injection techniques for enhanced shale gas recovery: Prospect and challenges.* Journal of Natural Gas Science and Engineering, 2020: p. 103240.

[159] Huneker, R., *Natural Gas Production and CO2 Sequestration in a Class 2 Hydrate Accumulation: A Numerical Simulation Study.* 2010.

[160] Li, S., et al., *Strategies for gas production from Class 2 hydrate accumulations by depressurization.* Fuel, 2021. **286**: p. 119380.

[161] Sun, Z., et al., *Numerical Simulation of the Depressurization Process of a Natural Gas Hydrate Reservoir: An Attempt at Optimization of Field Operational Factors with Multiple Wells in a Real 3D Geological Model.* Energies, 2016. **9**(9): p. 714.

[162] Liu, Y., et al., *Parameter optimization of Depressurization−to−Hot−Water−Flooding in heterogeneous hydrate bearing layers based on the particle swarm optimization algorithm.* Journal of Natural Gas Science and Engineering, 2018. **53**: p. 403-415.

[163] Sridhara, P., et al., *Novel Technological Approach To Enhance Methane Recovery from Class 2 Hydrate Deposits by Employing CO2 Injection.* Energy & Fuels, 2018. **32**(3): p. 2949-2961.

[164] Kurihara, M., et al. *Analysis of the JOGMEC/NRCan/Aurora Mallik gas hydrate production test through numerical simulation*. in *Proceedings of the 6th International Conference on Gas Hydrates, Vancouver, CANADA*. 2008.

[165] Khetan, A., M.K. Das, and K. Muralidhar, *Analysis of methane production from a porous reservoir via simultaneous depressurization and CO 2 sequestration.* Special Topics & Reviews in Porous Media: An International Journal, 2013. **4**(3).

[166] Song, Y., et al., *Evaluation of gas production from methane hydrates using depressurization, thermal stimulation and combined methods.* Appl. Energy, 2015. **145**: p. 265.

[167] Moridis, G.J., et al., *Numerical studies of gas production from several CH4 hydrate zones at the Mallik site, Mackenzie Delta, Canada.* Journal of petroleum science and engineering, 2004. **43**(3-4): p. 219-238.

[168] Moridis, G., et al., *Analysis and interpretation of the thermal test of gas hydrate dissociation in the JAPEX/JNOC/GSC et al. Mallik 5L-38 gas hydrate production research well.* 2005.

[169] Li, G., et al., *The use of huff and puff method in a single horizontal well in gas production from marine gas hydrate deposits in the Shenhu Area of South China Sea.* Journal of Petroleum Science and Engineering, 2011. **77**(1): p. 49-68.

[170] Chen, L., et al., *Numerical analysis of core-scale methane hydrate dissociation dynamics and multiphase flow in porous media.* Chemical Engineering Science, 2016. **153**: p. 221-235.

[171] Chen, L., et al., *Investigation on the dissociation flow of methane hydrate cores: numerical modeling and experimental verification.* Chemical Engineering Science, 2017. **163**: p. 31-43.

[172] Jin, G., et al., *Numerical evaluation of the methane production from unconfined gas hydrate-bearing sediment by thermal stimulation and depressurization in Shenhu area, South China Sea.* Journal of Natural Gas Science and Engineering, 2016. **33**: p. 497-508.

[173] Zhong, X., et al., *Evaluation of the gas production enhancement effect of hydraulic fracturing on combining depressurization with thermal stimulation from challenging ocean hydrate reservoirs.* Journal of Natural Gas Science and Engineering, 2020. **83**: p. 103621.

[174] Li, X.-S., et al., *Numerical simulation of gas production potential from permafrost hydrate deposits by huff and puff method in a single horizontal well in Qilian Mountain, Qinghai province.* Energy, 2012. **40**(1): p. 59-75.

[175] Moridis, G.J., et al., *Feasibility of gas production from a gas hydrate accumulation at the UBGH2-6 site of the Ulleung basin in the Korean East Sea.* Journal of Petroleum Science and Engineering, 2013. **108**: p. 180-210.

[176] Bei, K., et al., *Numerical Modeling of Gas Migration and Hydrate Formation in Heterogeneous Marine Sediments.* Journal of Marine Science and Engineering, 2019. **7**(10): p. 348.

[177] Zatsepina, O., M. Pooladi-Darvish, and H. Hong, *Behavior of gas production from Type III hydrate reservoirs.* Journal of Natural Gas Science and Engineering, 2011. **3**(3): p. 496-504.

[178] Huang, Y.-J., C.-Y. Wu, and B.-Z. Hsieh, *Effect of Fluid Saturation on Gas Recovery from Class-3 Hydrate Accumulations Using Depressurization: A Case Study of the Yuan-an Ridge Site in Southwestern Offshore Taiwan.* Energy Procedia, 2016. **97**: p. 310-317.

[179] Yang, S., et al., *Numerical simulation of Class 3 hydrate reservoirs exploiting using horizontal well by depressurization and thermal co-stimulation.* Energy Conversion and Management, 2014. **77**: p. 298-305.

[180] Merey, S. and C. Sinayuc, *Numerical simulations for short-term depressurization production test of two gas hydrate sections in the Black Sea.* Journal of Natural Gas Science and Engineering, 2017. **44**: p. 77-95.

[181] Uchida, S., A. Klar, and K. Yamamoto, *Sand production model in gas hydrate-bearing sediments.* International Journal of Rock Mechanics and Mining Sciences, 2016. **86**: p. 303-316.

[182] Anderson, B.J., et al., *Regional long-term production modeling from a single well test, Mount Elbert Gas Hydrate Stratigraphic Test Well, Alaska North Slope.* Marine and Petroleum Geology, 2011. **28**(2): p. 493-501.

[183] Li, X.-S., et al., *Numerical simulation of gas production from natural gas hydrate using a single horizontal well by depressurization in Qilian Mountain permafrost.* Industrial & engineering chemistry research, 2012. **51**(11): p. 4424-4432.

[184] Uddin, M., F. Wright, and D.A. Coombe, *Numerical Study of Gas Evolution and Transport Behaviours in Natural Gas-Hydrate Reservoirs.* Journal of Canadian Petroleum Technology, 2011. **50**(01): p. 70-89.

[185] Hong, H., M. Pooladi-Darvish, and P.R. Bishnoi, *Analytical Modelling of Gas Production From Hydrates in Porous Media.* Journal of Canadian Petroleum Technology, 2003. **42**(11): p. 45-56.

[186] Yu, T., et al., *3D investigation of the effects of multiple-well systems on methane hydrate production in a low-permeability reservoir.* Journal of Natural Gas Science and Engineering, 2020. **76**: p. 103213.

[187] Li, B., et al., *Depressurization induced gas production from hydrate deposits with low gas saturation in a pilot-scale hydrate simulator.* Applied Energy, 2014a. **129**: p. 274-286.

[188] Li, B., et al., *Kinetic Behaviors of Methane Hydrate Formation in Porous Media in Different Hydrate Deposits.* Industrial & Engineering Chemistry Research, 2014b. **53**(13): p. 5464-5474.

[189] Li, G., et al., *Methane hydrate dissociation using inverted five-spot water flooding method in cubic hydrate simulator.* Energy, 2014c. **64**: p. 298-306.

[190] Feng, Y., et al., *Numerical analysis of gas production from layered methane hydrate reservoirs by depressurization.* Energy, 2019. **166**: p. 1106-1119.

[191] Yu, T., G. Guan, and A. Abudula, *Production performance and numerical investigation of the 2017 offshore methane hydrate production test in the Nankai Trough of Japan.* Applied Energy, 2019a. **251**: p. 113338.

[192] Yu, T., et al., *Gas recovery enhancement from methane hydrate reservoir in the Nankai Trough using vertical wells.* Energy, 2019b. **166**: p. 834-844.

[193] Sun, Y., et al., *Numerical simulation of the short- and long-term production behavior of the first offshore gas hydrate production test in the South China Sea.* Journal of Petroleum Science and Engineering, 2019. **181**: p. 106196.

[194] Giraldo, C., et al., *Sensitivity analysis of parameters governing the recovery of methane from natural gas hydrate reservoirs.* Energies, 2014. **7**(4): p. 2148-2176.

[195] Vishal, V., et al., *Sensitivity analysis of methane hydrate bearing Class 3 reservoirs during thermal injection.* Journal of Petroleum Science and Engineering, 2020. **195**: p. 107575.

[196] Collett, T.S. and G.D. Ginsburg, *Gas Hydrates In the Messoyakha Gas Field of the West Siberian Basin - A Re-Examination of the Geologic Evidence.* International Journal of Offshore and Polar Engineering, 1998. **8**(01).

[197] Zhu, H., et al., *Numerical analysis of sand production during natural gas extraction from unconsolidated hydrate-bearing sediments.* Journal of Natural Gas Science and Engineering, 2020. **76**: p. 103229.

[198] Moridis, G.J., *Numerical Studies of Gas Production From Class 2 and Class 3 Hydrate Accumulations at the Mallik Site, Mackenzie Delta, Canada.* SPE Reservoir Evaluation & Engineering, 2004b. **7**(03): p. 175-183.

[199] Chong, Z.R., et al., *Review of natural gas hydrates as an energy resource: Prospects and challenges.* Applied Energy, 2016. **162**: p. 1633-1652.

[200] Boswell, R., et al., *The Iġnik Sikumi Field Experiment, Alaska North Slope: Design, Operations, and Implications for CO2–CH4 Exchange in Gas Hydrate Reservoirs.* Energy & Fuels, 2017a. **31**(1): p. 140-153.

[201] Boswell, R., *IġnIk SIkumI GaS Hydrate FIeld trIal Completed.* Natural Gas & Oil, 2012. **304**: p. 285-4541.

[202] Boswell, R., et al., *The Iġnik-Sikumi field experiment, Alaska North Slope: design, operations, and implications for CO2-CH4 exchange in gas hydrate reservoirs.* Energy Fuels, 2017b. **31**: p. 140.

[203] Schoderbek, D., et al., *North Slope Hydrate Fieldtrial: CO2/CH4 Exchange*, in *OTC Arctic Technology Conference*. 2012, Offshore Technology Conference: Houston, Texas, USA. p. 17.

[204] Yu, T., et al., *Application of horizontal wells to the oceanic methane hydrate production in the Nankai Trough, Japan.* Journal of Natural Gas Science and Engineering, 2019c. **62**: p. 113-131.

[205] Yu, T., et al., *Heat-assisted production strategy for oceanic methane hydrate development in the Nankai Trough, Japan.* Journal of Petroleum Science and Engineering, 2019d. **174**: p. 649-662.

[206] Sloan, E.D., *Fundamental principles and applications of natural gas hydrates.* Nature, 2003. **426**(6964): p. 353-359.

[207] Yu, T., et al., *Numerical investigation on the long-term gas production behavior at the 2017 Shenhu methane hydrate production site.* Applied Energy, 2021. **285**: p. 116466.

Highlights

- In all classes, combined methods were the most effective in producing methane
- CH_4 production in all classes depend on permeability pressure drop and temperature
- Simulators such as CMG STARS and TOUGH+HYDRATE provided better hydrate prediction results.
- Simulation results correlated with field studies results.
- Challenges are sand production, hydrate reformation, and rise of bottom well pressure

Declaration of interests

☒ The authors declare that they have no known competing financial interests or personal relationships that could have appeared to influence the work reported in this paper.

☐The authors declare the following financial interests/personal relationships which may be considered as potential competing interests:

We declare no conflict of interest.